



# **TWO DIMENSIONAL FRACTURE PROPAGATION CODE**

**(VERSION 1.1)**

**USER'S MANUAL**

Baotang Shen

FRACOM Ltd.  
[info@fracom.com.fi](mailto:info@fracom.com.fi)

## **ABSTRACT**

A two-dimensional boundary element code has been developed to simulate fracture initiation and propagation in an elastic and isotropic rock medium. The current version of the code is fully Window based and user friendly. The code can simulate up to 10-15 non-symmetrical, and randomly distributed fractures.

This manual provides: (a) the basic theoretical background of the FRACOD code; and (b) a detailed instruction on how to use the code. A number of simple examples are provided at the end of the report to demonstrate the applicability of the code.

The current version of the FRACOD code was developed based on a Ph.D. research (Shen, 1993). Further work on the code was conducted during 1998-2001, supported by SKB, Fracom Ltd and Tekes. It was designed to simulate fracture propagation in hard rocks.

# TABLE OF CONTENTS

	<b>ABSTRACT</b>	<b>i</b>
<b>1</b>	<b>INTRODUCTION</b>	<b>1</b>
<b>2</b>	<b>THEORETICAL BACKGROUND</b>	<b>2</b>
2.1	DISPLACEMENT DISCONTINUITY METHOD (DDM)	2
2.1.1	DISPLACEMENT DISCONTINUITY METHOD IN AN INFINITE SOLID	2
2.1.2	NUMERICAL PROCEDURE	3
2.2	SIMULATION OF ROCK DISCONTINUITIES	6
2.3	FRACTURE PROPAGATION CRITERION	8
2.4	DETERMINATION OF FRACTURE PROPAGATION USING DDM	10
2.5	FRACTURE INITIATION CRITERION	11
<b>3</b>	<b>CODE STRUCTURE</b>	<b>16</b>
<b>4</b>	<b>PREPARE INPUT FILE</b>	<b>19</b>
<b>5</b>	<b>CONDUCT AND MONITOR THE CALCULATION</b>	<b>24</b>
	<b>REFERENCES</b>	<b>35</b>
	<b>ACKNOWLEDGEMENTS</b>	<b>38</b>
	<b>APPENDIX I – HOW TO USE THE PREPROCESSOR TO SET UP MODELS</b>	<b>39</b>
	<b>APPENDIX II – VERIFICATION AND APPLICATION OF FRACOD</b>	<b>43</b>
	<b>APPENDIX III – DETERMINATION OF THE DIRECTION OF SHEAR FRACTURES</b>	<b>69</b>

# **1 INTRODUCTION**

Fracture propagation code (FRACOD) is a two-dimensional computer code that was designed to simulate fracture initiation and propagation in elastic and isotropic rock mediums. The code employs the Boundary Element Method (BEM) principles and a newly proposed fracture propagation criterion for detecting the possibility and the path of a fracture propagation, Shen and Stephansson (1993).

The current version of the FRACOD code provides the basic functions needed for studying rock fracture propagation in a rock mass subjected to far-field stresses. The code is created for running on PCs with a MS Windows 95/98/NT/2000 platform. It provides an easy-to-use user's interface that enables users to monitor and interrupt the calculation. It also provides an independent pre-processor to help users in preparing the input file for a given problem.

The capacity of the current version of the FRACOD code is limited to about 10-15 fractures, depending upon the complexity of the fracture system and the excavation. As a general estimate, a fracture system with 10 non-symmetrical fractures will require about 24 hours of calculation on a PC/400MHz to get a reasonably accurate prediction of fracture propagation.

This user's manual provides some basic theoretical background of the code in Chapters 2 and 3, and a detailed instruction on how to use the code in Chapters 4 and 5. Appendix I describes a pre-processor of the FRACOD code, while Appendix II gives ten simple application examples of using the FRACOD code. For those who may be only interested in knowing how to use the code rather than the theory, it is recommended to ignore Chapters 2 and 3 and start reading from Chapter 4.

## 2 THEORETICAL BACKGROUND

The FRACOD code is based on the Boundary Element Method principals. It utilises the Displacement Discontinuity Method (DDM), one of the three commonly used boundary element methods. In the FRACOD code, a newly proposed fracture criterion, the modified G-criterion (Shen and Stephansson, 1993), is incorporated into the numerical method for simulating fracture propagation. This section describes in detail the numerical method DDM as well as the modified G-criterion.

### 2.1 DISPLACEMENT DISCONTINUITY METHOD (DDM)

A crack or fracture has two surfaces or boundaries, one effectively coinciding with the other. Conventional boundary element methods, such as the Direct Integration Method, therefore become inefficient in simulating this problem. The Displacement Discontinuity Method (DDM) was developed by Crouch (1976) to cope with problems of this type. The DDM is based on the analytical solution to the problem of a constant discontinuity in displacement over a finite line segment in the  $x, y$  plane of an infinite and elastic solid. Physically, one may imagine a displacement discontinuity as a line crack whose opposing surfaces have been displaced relative to one another (see Figure 2-1.)

#### 2.1.1 Displacement Discontinuity Method in an infinite solid

The problem of a constant displacement discontinuity over a finite line segment in the  $x, y$  plane of an infinite elastic solid is specified by the condition that the displacements be continuous everywhere except over the line segment in question. The line segment may be chosen to occupy a certain portion of the  $x$ -axis, say the portion  $|x| \leq a, y=0$ . If we consider this segment to be a line crack, we can distinguish its two surfaces by saying that one surfaces is on the **positive** side of  $y=0$ , denoted  $y=0_+$ , and the other is on the **negative** side, denoted  $y=0_-$ . In crossing from one side of the line segment to the other, the displacement undergoes a constant specified change in value  $D_i = (D_x, D_y)$ .

We will define the displacement discontinuity  $D_i$  as the difference in displacement between the two sides of the segment as follows:

$$\begin{aligned} D_x &= u_x(x, 0_-) - u_x(x, 0_+) \\ D_y &= u_y(x, 0_-) - u_y(x, 0_+) \end{aligned} \tag{2-1}$$

Because  $u_x$  and  $u_y$  are positive in positive  $x$  and  $y$  co-ordinate direction, it follows that the  $D_x$  and  $D_y$  are positive as illustrated in Figure 2-1.

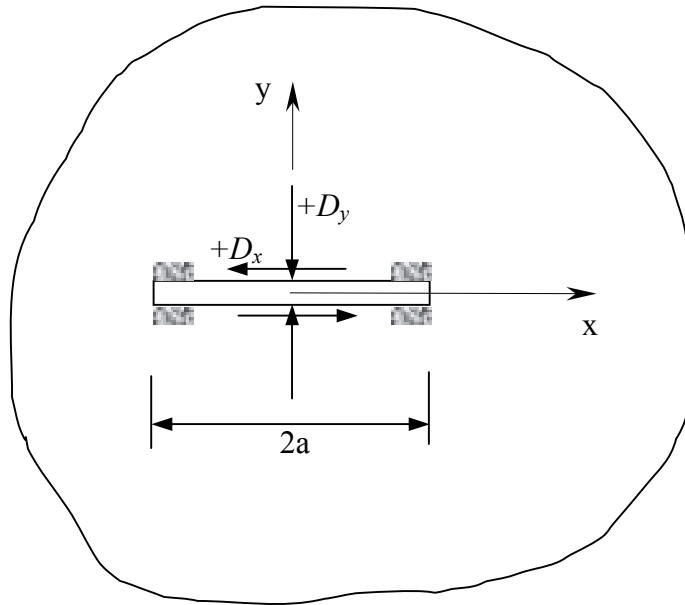


**Figure 2-1.** Constant displacement discontinuity components  $D_x$  and  $D_y$ .

The solution of the subject problem is given by Crouch (1976) and Crouch and Starfield (1983). The displacement and stresses can be written as:

$$\begin{aligned} u_x &= D_x [2(1-\nu)f_{,y} - yf_{,xx}] + D_y [-(1-2\nu)f_{,x} - yf_{,xy}] \\ u_y &= D_x [(1-2\nu)f_{,x} - yf_{,xy}] + D_y [2(1-\nu)f_{,y} - yf_{,yy}] \end{aligned} \quad 2-2$$

and

$$\begin{aligned} \sigma_{xx} &= 2GD_x [2f_{,xy} + yf_{,xyy}] + 2GD_y [f_{,yy} + yf_{,yyy}] \\ \sigma_{yy} &= 2GD_x [-yf_{,xyy}] + 2GD_y [f_{,yy} - yf_{,yyy}] \\ \sigma_{xy} &= 2GD_x [f_{,yy} + yf_{,yyy}] + 2GD_y [-yf_{,xyy}] \end{aligned} \quad 2-3$$

where  $f_{,x}$  represent the derivative of function  $f(x,y)$  against  $x$ , similarly as for  $f_{,y}, f_{,xy}, f_{,xxy}$  etc. Function  $f(x,y)$  in these equations is given by:

$$\begin{aligned} f(x,y) &= \frac{-1}{4\pi(1-\nu)} \left[ y \left( \arctan \frac{y}{x-a} - \arctan \frac{y}{x+a} \right) \right. \\ &\quad \left. - (x-a) \ln \sqrt{(x-a)^2 + y^2} + (x+a) \ln \sqrt{(x+a)^2 + y^2} \right] \end{aligned} \quad 2-4$$

### 2.1.2 Numerical procedure

For a crack of any shape, such as curved, we assume it can be represented with sufficient accuracy by  $N$  straight segments, joined end by end. The positions of the segments are specified with reference to the  $x, y$  co-ordinate

system shown in Figure 2-2. If the surface of the crack are subjected to stress (for example, a uniform fluid pressure  $-p$ ), they will displace relative to one another. The displacement discontinuity method is a means of finding a discrete approximation to the smooth distribution of relative displacement that exists in reality. The discrete approximation is found with reference to the  $N$  subdivisions of the crack depicted in Figure 2-2a. Each of the subdivisions is a boundary element and represents an elemental displacement discontinuity.

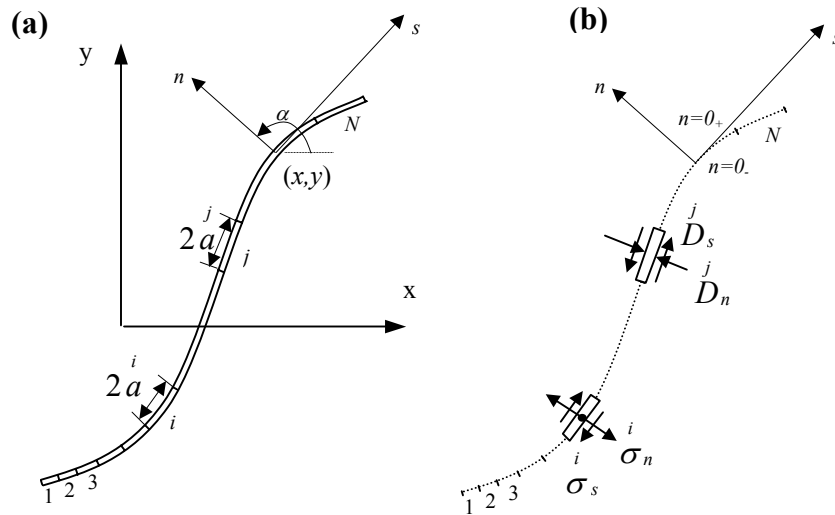


**Figure 2-2.** Representation of a crack by  $N$  elemental displacement discontinuities.

The elemental displacement discontinuities are defined with respect to the local co-ordinates  $s$  and  $n$  indicated in Figure 2-2. Figure 2-2b depicts a single elemental displacement discontinuity at  $j$ th segment of the crack. The components of discontinuity in the  $s$  and  $n$  directions at this segment are denoted as  $D_s^j$  and  $D_n^j$ . These quantities are defined as follows:

$$\begin{aligned}
 D_s^j &= u_s^- - u_s^+ \\
 D_n^j &= u_n^- - u_n^+
 \end{aligned}
 \tag{2-5}$$

In these definitions,  $u_s^j$  and  $u_n^j$  refer to the shear ( $s$ ) and normal ( $n$ ) displacement of the  $j$ th segment of the crack. The superscripts '+' and '-' denote the positive and negative surfaces of the crack with respect to local co-ordinate  $n$ .

The local displacements  $u_s^j$  and  $u_n^j$  form the two components of a vector. They are positive in the positive direction of  $s$  and  $n$ , irrespective of whether we are considering the positive or negative surface of the crack. As a consequence, it follows from Equation 2-5 that the normal component of

displacement discontinuity  $\overset{j}{D}_n$  is positive if the two surfaces of the crack displace toward one another. Similarly, the shear component  $\overset{j}{D}_s$  is positive if the positive surface of the crack moves to the left with respect to the negative surface.

The effects of a single elemental displacement discontinuity on the displacements and stresses at an arbitrary point in the infinite solid can be computed from the results for section 2.1.1, provided we suitably transform the equations to account for the position and orientation of the line segment in question. In particular, the shear and normal stresses at the midpoint of the  $i$ th element in Figure 2-2b can be expressed in terms of the displacement discontinuity components at the  $j$ th element as follows:

$$\left. \begin{aligned} \sigma_s^i &= A_{ss}^{ij} \overset{j}{D}_s + A_{sn}^{ij} \overset{j}{D}_n \\ \sigma_n^i &= A_{ns}^{ij} \overset{j}{D}_s + A_{nn}^{ij} \overset{j}{D}_n \end{aligned} \right\} i=1 \text{ to } N \quad 2-6$$

where  $A_{ss}^{ij}$ , etc., are the boundary influence coefficients for the stresses. The coefficient  $A_{ns}^{ij}$ , for example, gives the normal stress at the midpoint of the  $i$ th element (i.e.  $\sigma_n^i$ ) due to a constant unit shear displacement discontinuity over the  $j$ th element (i.e.  $\overset{j}{D}_s=1$ ).

Returning now to the crack problem depicted in Figure 2-2b, we place an elemental displacement discontinuity at each of the  $N$  segments along the crack and write, from Equation 2-6,

$$\left. \begin{aligned} \sigma_s^i &= \sum_{j=1}^N A_{ss}^{ij} \overset{j}{D}_s + \sum_{j=1}^N A_{sn}^{ij} \overset{j}{D}_n \\ \sigma_n^i &= \sum_{j=1}^N A_{ns}^{ij} \overset{j}{D}_s + \sum_{j=1}^N A_{nn}^{ij} \overset{j}{D}_n \end{aligned} \right\} i=1 \text{ to } N \quad 2-7$$

If we specify the values of the stress  $\overset{j}{\sigma}_s$  and  $\overset{j}{\sigma}_n$  for each element of the crack, then Equation 2-7 is a system of  $2N$  simultaneous linear equations in  $2N$  unknowns, namely the elemental displacement discontinuity components  $\overset{j}{D}_s$  and  $\overset{j}{D}_n$ . We can find the displacements and stresses at designated points in the body by using the principle of superposition. In particular, the displacements along the crack of Figure 2-2a are given by expressions of the form

$$\left. \begin{aligned} u_s^i &= \sum_{j=1}^N B_{ss}^{ij} D_s^j + \sum_{j=1}^N B_{sn}^{ij} D_n^j \\ u_n^i &= \sum_{j=1}^N B_{ns}^{ij} D_s^j + \sum_{j=1}^N B_{nn}^{ij} D_n^j \end{aligned} \right\} i=1 \text{ to } N \quad 2-8$$

where  $B_{ss}^{ij}$ , etc., are the boundary influence coefficients for the displacements. The displacements are discontinuous when passing from one side of the  $j$ th element to the other, so we must distinguish between these two sides when computing the influence coefficients in Equation 2-8. The diagonal terms of the influence coefficients in these equations have the values

$$\begin{aligned} B_{sn}^{ij} &= B_{ns}^{ij} = 0 \\ B_{ss}^{ij} &= B_{nn}^{ij} = -\frac{1}{2}(n \rightarrow 0_+); +\frac{1}{2}(n \rightarrow 0_-); \end{aligned} \quad 2-9$$

The remaining coefficients (i.e. the ones for which  $i \neq j$ ) are continuous and they can be obtained by using Equations 2-1, 2-2 and 2-3 in Section 2.1.1. Displacements  $u_s^i$  and  $u_n^i$  in Equation 2-8 will exhibit constant discontinuities  $D_s^i$  and  $D_n^i$ , as required.

## 2.2 SIMULATION OF ROCK DISCONTINUITIES

For a rock discontinuity (crack, joint, etc.) in an infinite elastic rock mass, the system of governing equations 2-7 can be written as

$$\left. \begin{aligned} \sigma_s^i &= \sum_{j=1}^N A_{ss}^{ij} D_s^j + \sum_{j=1}^N A_{sn}^{ij} D_n^j - (\sigma_s)_0^i \\ \sigma_n^i &= \sum_{j=1}^N A_{ns}^{ij} D_s^j + \sum_{j=1}^N A_{nn}^{ij} D_n^j - (\sigma_n)_0^i \end{aligned} \right\} i=1 \text{ to } N \quad 2-10$$

where  $\sigma_s^i$  and  $\sigma_n^i$  represent the shear and normal stresses of the  $i$ th element respectively;  $(\sigma_s)_0^i, (\sigma_n)_0^i$  are the far-field stresses transformed in the crack shear and normal directions.  $A_{ss}^{ij}, \dots, A_{nn}^{ij}$  are the influence coefficients, and  $D_s^j, D_n^j$  represent displacement discontinuities of  $j$ th element which are unknowns in the system of equations.

A rock discontinuity has three states: open, in elastic contact or sliding. The system of governing equations 2-10, developed for an open crack, can be

easily extended to the case for cracks in contact and sliding. For different crack states, their system of governing equations can be rewritten in the following ways, depending on the shear and normal stresses ( $\sigma_s^i$  and  $\sigma_n^i$ ) of the crack.

- For an open crack  $\sigma_s^i = \sigma_n^i = 0$ , therefore the system of governing equations 2-10 can be rewritten as:

$$\left. \begin{aligned} \sigma_s^i = 0 &= \sum_{j=1}^N A_{ss}^{ij} D_s^j + \sum_{j=1}^N A_{sn}^{ij} D_n^j - (\sigma_s^i)_0 \\ \sigma_n^i = 0 &= \sum_{j=1}^N A_{ns}^{ij} D_s^j + \sum_{j=1}^N A_{nn}^{ij} D_n^j - (\sigma_n^i)_0 \end{aligned} \right\} i=1 \text{ to } N \quad 2-11$$

- When the two crack surfaces are in elastic contact, the magnitude of  $\sigma_s^i$  and  $\sigma_n^i$  will depend on the crack stiffness ( $K_s, K_n$ ) and the displacement discontinuities ( $D_s^j, D_n^j$ )

$$\begin{aligned} \sigma_s^i &= K_s D_s^i \\ \sigma_n^i &= K_n D_n^i \end{aligned} \quad 2-12$$

where  $K_s$  and  $K_n$  are the crack shear and normal stiffness, respectively. Substituting Equation 2-12 into Equation 2-10 and carrying out the simple mathematical manipulation, the system of governing equations then becomes:

$$\left. \begin{aligned} 0 &= \sum_{j=1}^N A_{ss}^{ij} D_s^j + \sum_{j=1}^N A_{sn}^{ij} D_n^j - (\sigma_s^i)_0 - K_s D_s^i \\ 0 &= \sum_{j=1}^N A_{ns}^{ij} D_s^j + \sum_{j=1}^N A_{nn}^{ij} D_n^j - (\sigma_n^i)_0 - K_n D_n^i \end{aligned} \right\} i=1 \text{ to } N \quad 2-13$$

- For a crack with its surfaces sliding

$$\begin{aligned} \sigma_n^i &= K_n D_n^i \\ \sigma_s^i &= \pm \sigma_n^i \tan \phi = \pm K_n D_n^i \tan \phi \end{aligned} \quad 2-14$$

where  $\phi$  is the friction angle of the crack surfaces. The sign of  $\sigma_s^i$  depends on the sliding direction. Consequently, the system of equations 2-10 can be presented as:

$$\left. \begin{aligned}
 0 &= \sum_{j=1}^N A_{ss}^{ij} D_s^j + \sum_{j=1}^N A_{sn}^{ij} D_n^j - (\sigma_s)_0 \pm K_n D_n^i \tan \phi \\
 0 &= \sum_{j=1}^N A_{ns}^{ij} D_s^j + \sum_{j=1}^N A_{nn}^{ij} D_n^j - (\sigma_n)_0 - K_n D_n^i
 \end{aligned} \right\} i=1 \text{ to } N \quad 2-15$$

The displacement discontinuities ( $D_s^j, D_n^j$ ) of the crack are obtained by solving the system of governing equations using conventional numerical techniques, e.g. Gauss elimination method. If the crack is open the stresses ( $\sigma_s^i, \sigma_n^i$ ) on the crack surfaces are zero, otherwise if the crack is in contact or sliding, they can be calculated by Equations 2-12 or 2-14.

The state of each crack (joint) element can be determined using the Mohr-Coulomb failure criterion:

- (1) open joint:  $\sigma_n > 0$
- (2) elastic joint:  $\sigma_n < 0, |\sigma_s| < c + |\sigma_n| \tan \phi$
- (3) sliding joint:  $\sigma_n < 0, |\sigma_s| \geq c + |\sigma_n| \tan \phi$

where a compressive stress is taken to be negative and  $c$  is cohesion. If the joint has experienced sliding,  $c = 0$ .

### 2.3 FRACTURE PROPAGATION CRITERION

In modelling fracture propagation in rock masses where both tensile and shear failure are common, a fracture criterion for predicting both mode I and mode II fracture propagation is needed. The existing fracture criteria in the macro-approach can be classified into two groups: the principal stress (strain)-based criteria and the energy-based criteria. The first group consists of the Maximum Principal Stress Criterion and the Maximum Principal Strain Criterion; the second group includes the Maximum Strain Energy Release Rate Criterion (G-criterion) and the Minimum Strain Energy Density Criterion (S-criterion). The principal stress (strain)-based criteria are only applicable to the mode I fracture propagation which relies on the principal tensile stress (strain). To be applied for the mode II propagation, a fracture criterion has to consider not only the principal stress (strain) but also the shear stress (strain). From this point of view, the energy based criteria seem to be applicable for both mode I and II propagation because the strain energy in the vicinity of a fracture tip is related to all the components of stress and strain.

Both the G-criterion and the S-criterion have been examined for application to the mode I and mode II propagation (Shen and Stephansson, 1993), and neither of them is directly suitable. In a study by Shen and Stephansson (1993) the original G-criterion has been improved and extended. The

original G-criterion states that when the strain energy release rate in the direction of the maximum G-value reaches the critical value  $G_c$ , the fracture tip will propagate in that direction. It does not distinguish between mode I and mode II fracture toughness of energy ( $G_{Ic}$  and  $G_{IIc}$ ). In fact, for the most of the engineering materials, the mode II fracture toughness is much higher than the mode I toughness due to the differences in the failure mechanism. In rocks, for instance,  $G_{IIc}$  is found in laboratory scale to be at least two orders of magnitude higher than  $G_{Ic}$  (Li, 1991). Applied to the mixed mode I and mode II fracture propagation, the G-criterion is difficult to use since the critical value  $G_c$  must be carefully chosen between  $G_{Ic}$  and  $G_{IIc}$ .

A modified G-criterion, namely the F-criterion, was proposed (Shen and Stephansson, 1993). Using the F-criterion the resultant strain energy release rate ( $G$ ) at a fracture tip is divided into two parts, one due to mode I deformation ( $G_I$ ) and one due to mode II deformation ( $G_{II}$ ). Then the sum of their normalized values is used to determine the failure load and its direction.  $G_I$  and  $G_{II}$  can be expressed as follows (Figure 2-3): if a fracture grows an unit length in an arbitrary direction and the new fracture opens without any surface shear displacement, the strain energy loss in the surrounding body due to the fracture growth is  $G_I$ . Similarly, if the new fracture has only a surface shear displacement, the strain energy loss is  $G_{II}$ . The principles of the F-criterion can be stated as follows:

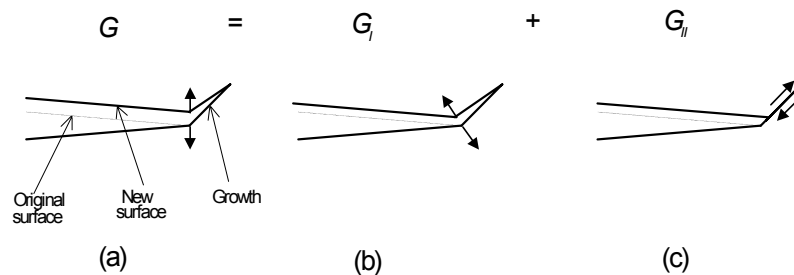


**Figure 2-3.** Definition of  $G_I$  and  $G_{II}$  for fracture growth. (a)  $G$ , the growth has both open and shear displacement; (b)  $G_I$ , the growth has only open displacement; (c)  $G_{II}$ , the growth has only shear displacement.

(1). In an arbitrary direction ( $\theta$ ) at a fracture tip there exists a F-value, which is calculated by

$$F(\theta) = \frac{G_I(\theta)}{G_{Ic}} + \frac{G_{II}(\theta)}{G_{IIc}} \tag{2-16}$$

(2). The possible direction of propagation of the fracture tip is the direction ( $\theta = \theta_0$ ) for which the F-value reaches its maximum.

$$F(\theta) \Big|_{\theta=\theta_0} = \max. \tag{2-17}$$

(3). When the maximum F-value reaches 1.0, the fracture tip will propagate, i.e.

$$F(\theta)\Big|_{\theta=\theta_0} = 1.0 \quad 2-18$$

The F-criterion is actually a more general form of the G-criterion and it allows us to consider mode I and mode II propagation simultaneously. In most cases, the F-value reaches its peak either in the direction of maximum tension ( $G_{Ic} = \text{maximum while } G_{IIc}=0$ ) or in the direction of maximum shearing ( $G_{IIc} = \text{maximum while } G_{Ic}=0$ ). This means that a fracture propagation of a finite length (the length of an element, for instance) is either pure mode I or pure mode II. However, the fracture growth may socialite between mode I and mode II during an ongoing process of propagation, and hence form a path which exhibits the mixed mode failure in general.

## 2.4 DETERMINATION OF FRACTURE PROPAGATION USING DDM

The key step in using the F-criterion is to determine the strain energy release rate of mode I ( $G_I$ ) and mode II ( $G_{II}$ ) at a given fracture tip. As  $G_I$  and  $G_{II}$  are only the special cases of  $G$ , the problem is then how to use DDM to calculate the strain energy release rate  $G$ .

The G-value, by definition, is the change of the strain energy in a linear elastic body when the crack has grown one unit of length. Therefore, to obtain the G-value the strain energy must first be estimated.

By definition, the strain energy,  $W$ , in a linear elastic body is

$$W = \iiint_V \frac{1}{2} \sigma_{ij} \varepsilon_{ij} dV . \quad 2-19$$

where  $\sigma_{ij}$  and  $\varepsilon_{ij}$  are the stress and strain tensors, and  $V$  is the volume of the body. The strain energy can also be calculated from the stresses and displacements along its boundary

$$W = \frac{1}{2} \int_S (\sigma_s u_s + \sigma_n u_n) ds \quad 2-20$$

where  $\sigma_s, \sigma_n, u_s, u_n$  are the stresses and displacements in tangential and normal direction along the boundary of the elastic body. Applying Equation 2-20 to the crack system in an infinite body with far-field stresses in the shear and normal direction of the crack,  $(\sigma_s)_0$  and  $(\sigma_n)_0$ , the strain energy,  $W$ , in the infinite elastic body is

$$W = \frac{1}{2} \int_0^a [(\sigma_s - (\sigma_s)_0) D_s + (\sigma_n - (\sigma_n)_0) D_n] da \quad 2-21$$

where  $a$  is the crack length,  $D_s$  is the shear displacement discontinuity and  $D_n$  is the normal displacement discontinuity of the crack. When DDM is used to calculate the stresses and displacement discontinuities of the crack, the strain energy can also be written in terms of the element length ( $a^i$ ) and the stresses and displacement discontinuities of the  $i$ th element of the crack.

$$W \approx \frac{1}{2} \sum_i (a^i (\sigma_s^i - (\sigma_s)_0) D_s + a^i (\sigma_n^i - (\sigma_n)_0) D_n) \quad 2-22$$

The G-value can be estimated by

$$G(\theta) = \frac{\partial W}{\partial a} \approx \frac{[W(a + \Delta a) - W(a)]}{\Delta a} \quad 2-23$$

where  $W(a)$  is the strain energy governed by the original crack while  $W(a + \Delta a)$  is the strain energy governed by both the original crack,  $a$ , and its small extension,  $\Delta a$  (Figure 2-4). In Figure 2-4, a 'fictitious' element is introduced to the tip of the original crack with the length  $\Delta a$  in the direction  $\theta$ . Both  $W(a)$  and  $W(a + \Delta a)$  can be determined easily by directly using DDM and Equation 2-23.

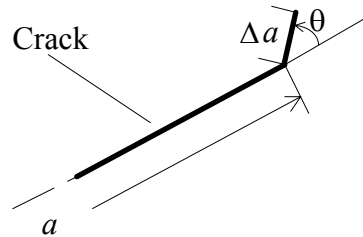


**Figure 2-4.** Fictitious crack increment  $\Delta a$  in direction  $\theta$  with respect to the initial crack orientation.

In the above calculation, if we restrict numerically the shear displacement of the “fictitious” element to zero, the result obtained using Equation 2-23 will be  $G_I(\theta)$ . Similarly, if we restrict the normal displacement of the “fictitious” element to zero, the result obtained will be  $G_{II}(\theta)$ . After obtaining both  $G_I(\theta)$  and  $G_{II}(\theta)$ , the F-value in Equation 2-16 can be calculated using the given fracture toughness values  $G_{Ic}$  and  $G_{IIc}$  of a given rock type.

## 2.5 FRACTURE INITIATION CRITERION

In addition to the propagation of existing fractures, new fractures (cracks) may initiate at the boundaries or in the intact rock. This section describes the criteria used to detect fracture initiation.

### Fracture initiation in intact rock

Fracture initiation is a complicated process. It often starts from microcrack formation. The microcracks coalesce and finally form macro-fractures. Because the FRACOD code is designed to simulate the fracturing process in macro-scale only, we ignore the process of microcrack formation. Rather, we will only focus on when and whether a macro-fracture will form at a given location with a given stress state.

The FRACOD code considers the intact rock as a flawless and homogeneous medium. Therefore, any fracture initiation from such a medium represents a localised failure of the intact rock. The localised failure can be predicted by an existing failure criterion, e.g. Mohr-Coulomb criterion. Other criteria widely used in rock mechanics and rock engineering can also be used, such as Hoek-Brown criterion etc.

A rock failure can be caused by tension or shear. Hence, a fracture initiation can be formed due to tension or shear. For tensile fracture initiation, the tensile failure criterion is used in FRACOD, i.e. when the tensile stress at a given point of the intact rock exceeds the tensile strength of the intact rock, a new rock fracture will be generated in the direction perpendicular to the tensile stress (Figure 2-5)

Critical stress of fracture initiation in tension:

$$\sigma_{\text{tensile}} \geq \sigma_t$$

Direction of fracture initiation in tension:

$$\theta_{\text{it}} = \theta(\sigma_{\text{tensile}}) + \pi/2$$

where  $\sigma_{\text{tensile}}$  is the principal tensile stress at a given point,  $\sigma_t$  is the tensile strength of the intact rock,  $\theta_{\text{it}}$  is the direction of the fracture initiation in tension, and  $\theta(\sigma_{\text{tensile}})$  is the direction of the tensile stress.

The length of the newly generated fracture is determined by the spacing of the grid points used in the intact rock. In the current FRACOD version, it is equal to the grid point spacing in the initiation direction. The less the grid point spacing, the shorter the new fracture. However, the closer the grid points, the less different the stresses at the adjacent grid points, and hence the more likely a fracture initiation occurs in the adjacent grid points simultaneously. The newly formed short fractures link with each other to form a longer fracture. This mechanism reduces the sensitivity of the modelling results to the grid point spacing.

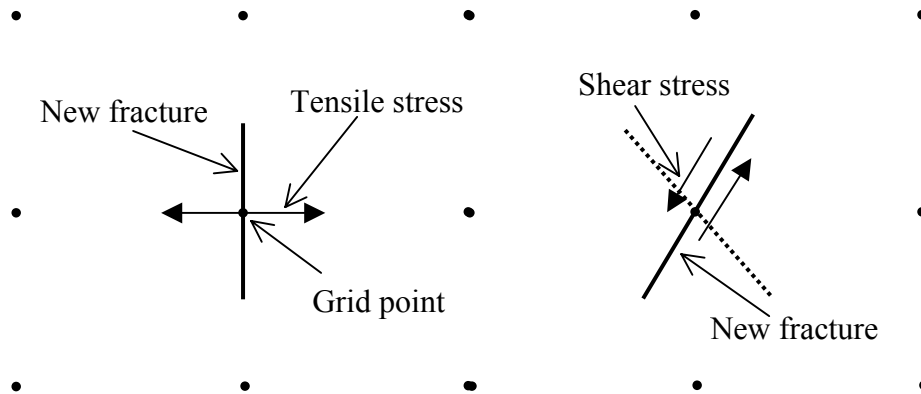


Figure 2-5. Fracture initiation in tension or shear in intact rock.

For a shear fracture initiation, the Mohr-Coulomb failure criterion is used in FRACOD, i.e. when the shear stress at a given point of the intact rock exceeds the shear strength of the intact rock, a new rock fracture will be generated (Figure 2-5)

Critical stress of fracture initiation in shear:

$$\sigma_{\text{shear}} \geq \sigma_n \tan(\phi) + c$$

Direction of fracture initiation in shear:

$$\theta_{\text{is}} = \phi/2 + \pi/4$$

where  $\sigma_{\text{tensile}}$  is the shear stress in the direction of  $\theta_{\text{is}}$ ,  $\sigma_n$  is the normal stress to the shear failure plane,  $\phi$  is the internal friction angle of intact rock,  $c$  is the cohesion, and  $\theta_{\text{is}}$  is the direction of potential shear failure, which is measured from the direction of the minimum principal stress.

Because there are always two symmetric shear failure planes at any given point, two fractures are added in the model whenever a shear failure is detected. Often one of the two fractures will propagate predominately in later simulation of fracture propagation.

The length of the shear fracture initiation depends upon the spacing of the grid points, as discussed above for the tensile fracture initiation.

Fracture initiation at boundaries

Fracture initiation at a boundary is not as a straight forward task as that in intact rock. Because the boundary may be a straight boundary, a curved boundary, or a boundary with sharp corners, significantly stress concentration may occur at the boundary. Recent study by Shen and Rinne (2001) has highlighted the complexity of the fracture initiation at boundaries. The initiation criteria suggested by Shen and Rinne (2001) may be suitable for the cases studied but not universally for all cases. There is no simple and yet theoretically sound methods for the prediction of fracture initiation from boundaries.

To enable the simulation of fracture propagation at boundary using FRACOD, an alternative approach is taken. Instead of directly predicting the fracture initiation from a boundary, we examine the fracture initiation from the intact rock very close to the boundary, using the intact rock failure criteria as discussed before. Once an intact rock failure is detected, a fracture initiation is predicted to occur in the intact rock close to the boundary. FRACOD then detects whether the newly formed fracture will link to the boundary by using the fracture propagation functions. This treatment fully utilises the advantage of the fracture propagation functions built in the code and overcomes the lack of effective methods in handling fracture initiation from the boundary.

New grid points are arranged in the intact rock along the boundary (Figure 2-6). They are set to be at a distance of one element away from the boundary since the constant DDM method does not give accurate results very close to the element. The grid points are effectively treated to be the same as other grid points in the intact rock, and the same procedure is used to detect any possible fracture initiation from these grid points. If a fracture initiation is predicted from any of the grid points close to the boundaries, a new fracture is created at the grid point in the direction of failure. The length of the fracture is a half of the length of the nearest boundary element. The code then detects whether the fracture will propagate to the boundary. If yes, the fracture will link to the boundary and effectively form a fracture initiation from the boundary.

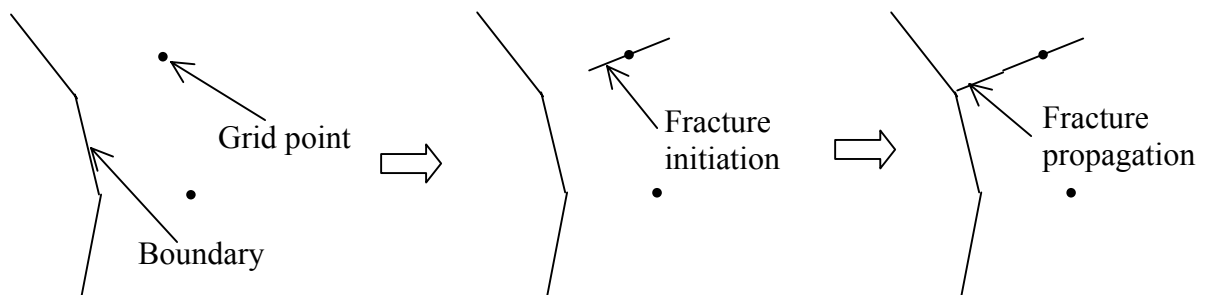
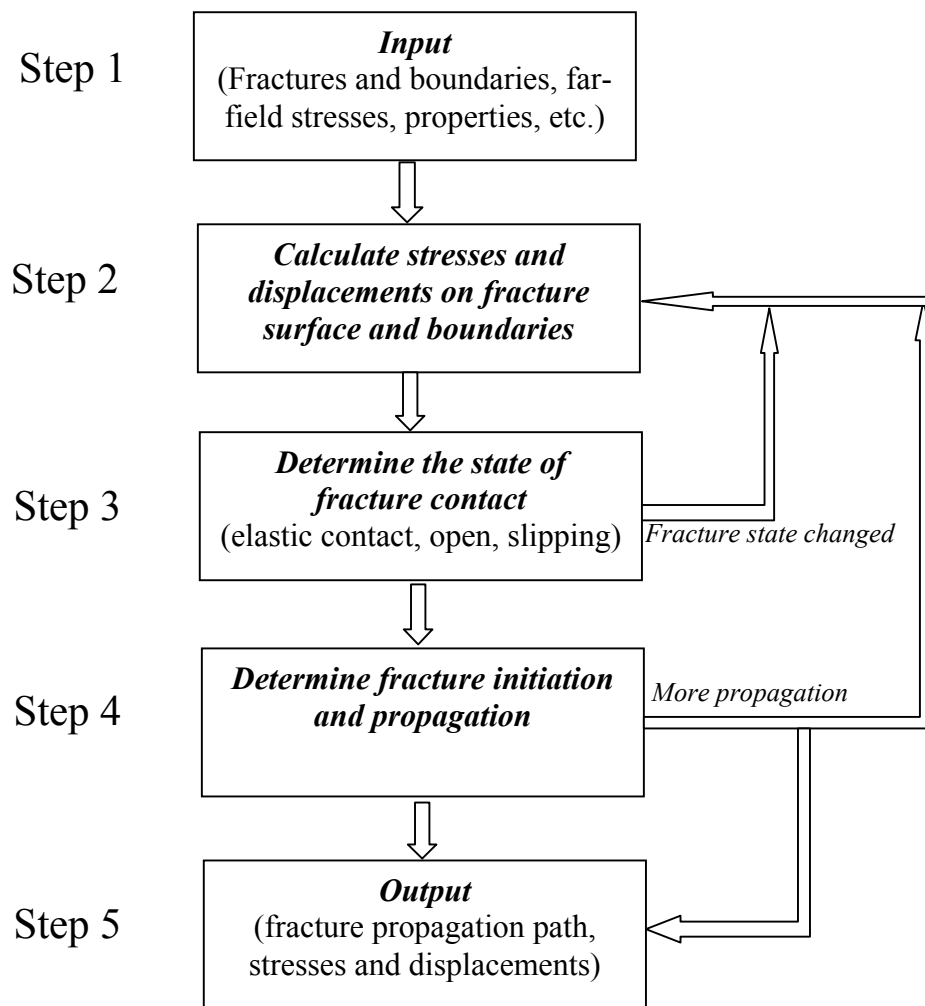


Figure 2.6. Modelling process of a fracture initiation from boundary.

An existing fracture is treated to be the same as a boundary. The same procedure is used to detect if any fracture initiation will occur close to the surface of a fracture. In case of a fracture, grid points will be added to both sides of the fracture surface since both sides are solid rock. The fracture initiation process does not apply to the tips of an existing fracture. At a fracture tip, stress singularity occurs and any intact rock failure criterion is no longer valid. The fracture propagation modelling procedure as described in Sections 2.1-2.4 is then used.

### 3 CODE STRUCTURE

The FRACOD code performs the fracture propagation calculation in a process shown by the program flow chart in Figure 3-1. Details of the key steps in the Figure 3-1 are described below.



**Figure 3-1.** Flow chart of the FRACOD code.

**Step 1: Input**

The code will read the input data from a pre-defined data file. The input data includes the geometry of pre-existing fractures and boundaries, far-field stresses, elastic properties of the rock mass, fracture toughnesses etc. A comprehensive description of the input data and their format are given in Chapter 4.

**Step 2: Calculation of stresses and displacements**

This is a standard routine using the DDM formulas described in Section 2.1 to calculate the stresses and displacements on fracture surfaces, boundaries and/or any pre-defined internal points in the rock mass.

**Step 3: Determination of the state of fracture contact**

The initial calculation of stresses and displacements using DDM is performed based on the assumption that all fractures are in surface elastic contact. This may not be true as fracture surfaces could be open or sliding as well. Therefore, a correction process is needed. This is done in a cyclic checking process. After obtaining the shear and normal stresses on each fracture element from the DDM calculation using the elastic fracture assumption, the code will check whether the open criterion or fracture sliding criterion is met for each fracture element. If yes, the new fracture states as determined will be assigned to the fracture elements, and a new cycle of DDM calculation will be performed using the updated states of fracture elements. The calculated shear and normal stresses on the fracture elements will again be used to check whether any change of state of fracture contact is detected. If yes, a new cycle of DDM calculation will be performed again. This cycling process will continue until no more change in fracture contact state is found and the results then are regarded to be the true results.

**Step 4: Determination of fracture initiation and propagation**

After obtaining the stresses and displacements on fractures and boundaries, the elastic strain energy,  $W(a)$ , is calculated. By adding a small fictitious element ( $\Delta a$ , normally the same length of the tip element) at a fracture tip, say, tip A, in the direction of  $\theta$ , a new strain energy,  $W(a+\Delta a)$ , can then be obtained. Using the formulas listed in Sections 2.3 and 2.4, the code then calculates the F-value for fracture tip A in the direction of  $\theta$ , i.e.  $F(\theta)$ . The direction  $\theta$  is then rotated from  $-180^\circ$  to  $+180^\circ$  with an defined interval to cover the whole direction range. The F-value at these directions is hence obtained. As described by the F-criterion, the direction where the F-value is the maximum will be the direction of a potential fracture growth. If the F-value in this direction is found to be equal to or greater than 1.0, a fracture propagation is detected for fracture tip A.

Similar process will be performed for all fracture tips. The tips found to have fracture propagation will, at the end of the detection process, be added with a new element in the direction of fracture propagation. The element will have the same length as the tip element.

After adding a new element to each fracture tip found to propagate, a new cycle of calculation in steps 2, 3 and 4 will be performed to find whether further fracture propagation will occur. If yes, the calculation cycle will

continue until there is no more fracture propagation or is stopped by the user.

Also detected in this step is the fracture initiation from intact rock, fracture surface and boundaries. If failure is detected at a grid points, new fractures will be added. The code will then treat the new fractures the same as other existing fractures and detects whether any fracture propagation will occur.

**Step 5: Output**

During the cyclic calculation, the geometry of propagating fractures and other boundaries are shown on the screen so that the user can monitor the calculation process. When the calculation is completed or is interrupted by the user, stresses and displacements, in addition to the fracture geometry, can be plotted on screen using the available options provided in the FRACOD program window. The screen plots can also be printed to printer or captured as image files which can then be directly pasted to other applications such as MS Word for reporting.

## 4 PREPARE INPUT FILE

The FRACOD code reads the input data from a data file previously prepared with specified formats. Therefore, the user needs to construct the input file (e.g. input.dat) before running the code. This section gives a detailed instruction on how to prepare the input file for the FRACOD code. The following is an example data file which defines a borehole with cracks in the borehole wall under uniaxial compression.

```

----- example data file -----
TITLE
A borehole with four cracks loaded in uniaxial compression
SYMMETRY -- Model symmetry
      4  0.00  0.00
MODULUS -- Poisson Ratio and Youngs modulus
      0.25  0.40E+11
TOUGHNESS -- Gic and Giic
      50.    1000.
PROPERTIES -- mat, kn, ks, phi, coh
      1  0.10E+13  0.10E+13  30.0  0.00E+00
SWINDOW -- xll,xur,yll,yur,numx,numy
      -3.00    3.00    -3.00    3.00  30  30
STRESSES -- sxx,syy,sxy
      0.00E+07  -0.15E+08  0.00E+00
FRACTURE -- nume,xbeg,ybeg,xend,yend,kode,mat
      5  0.700  0.700  1.000  1.000  2  1
ARCH -- nume,xcen,ycen,diam,ang1,ang2,kode,ss,sn
      10  0.0  0.0  2.0  0.0  90.0  1  0.00E+00
0.00E+00
CYCL 1000
ENDFILE
STOP
----- end of the example data file -----

```

The input data are defined by a command line, such as TITLE. The command line will, if needed, be followed by a line which defines the values. Only the first four characters of a command (e.g. TITL) are to be read by the code and hence meaningful. However, it is always desirable to write the whole word (e.g. TITLE) to help in understanding the function of this command.

All commands can be written in pure capital characters or pure small characters, or their mixture, such as "STOP", "stop", or "Stop". Unacceptable commands cause no action in the code (no warning or error messages will be given).

The commands used by the FRACOD code are listed below. Note that the units used for the input are given in brackets.

- TITL** give a title to the problem  
(*words within 80 letters*)
- SYMM** give symmetry conditions  
*ksym, xsym, ysym*
- ksym = 0 -- no symmetry*  
*ksym = 1 -- problem symmetrical against vertical line  $x=x_{sym}$  (m)*  
*ksym = 2 -- problem symmetrical against horizontal line  $y=y_{sym}$  (m)*  
*ksym = 3 -- problem symmetrical against point  $x=x_{sym}$  and  $y=y_{sym}$  (m)*  
*ksym = 4 -- problem symmetrical against line  $x=x_{sym}$  and line  $y=y_{sym}$  (m)*
- MODU** give elastic properties (modulus) of the rock medium  
 *$\nu$  (Poisson's ratio),  $E$  (Young's modulus) (Pa)*
- TOUG** give critical energy release rates  $G_{Ic}$  and  $G_{IIc}$
- $G_{Ic}$ ,  $G_{IIc}$*
- $G_{Ic}$  -- mode I fracture critical strain energy release rate ( $J\ m^{-2}$ )*
- $$G_{Ic} = (1 - \nu^2) K_{Ic}^2 / E \quad (K_{Ic} - \text{Fracture toughness mode I})$$
- $G_{IIc}$  -- mode II fracture critical strain energy release rate ( $J\ m^{-2}$ )*
- $$G_{IIc} = (1 - \nu^2) K_{IIc}^2 / E \quad (K_{IIc} - \text{Fracture toughness mode II})$$
- PROP** give fracture surface contact properties
- jmat, ks, kn, phi, coh*
- jmat* -- joint property ID (1,2,3,...)  
*ks* -- fracture shear stiffness (Pa/m)  
*kn* -- fracture normal stiffness (Pa/m)  
*phi* -- fracture friction angle (degree)  
*coh* -- fracture cohesion (Pa)
- ROCK** give intact rock strength parameters for fracture initiation
- rphi, rcoh, sigt*
- rphi* – Intact rock internal friction angle (degrees)  
*rcoh* – Intact rock cohesion (Pa)  
*sigt* – Intact rock tensile strength (Pa)
- SWIN** define a window for plotting the geometry, stresses and displacements
- xll, xur, yll, yur, numx, numy*

*xll* -- left border of the window (m)  
*xur* -- right border of the window (m)  
*yll* -- bottom border of the window (m)  
*yur* -- top border of the window (m)  
*numx* -- number of grid points along x-direction  
*numy* -- number of grid points along y-direction

**IWIN** define an area window for detecting fracture initiation (used only when once particular problem area is of interests)

***xmin, xmax, ymin, ymax***

*xmin* -- left border of the window (m)  
*xmax* -- right border of the window (m)  
*ymin* -- bottom border of the window (m)  
*ymax* -- top border of the window (m)

**STRE** give far-field stresses in the rock mass

***Pxx, Pyy, Pxy***

*Pxx* – Far-field horizontal stress (Pa)  
*Pyy* – Far-field vertical stress (Pa)  
*Pxy* – Far-field shear stress (Pa)

Warning: if *Pxy* is not 0, only *ksym=0* or *ksym = 3* may be used.

**FRAC** define a fracture (joint)

***num, xbeg, ybeg, xend, yend, kode, jmat***

*num* -- number of elements along the fracture  
*(xbeg, ybeg)* – co-ordinates of the beginning point of the fracture (m)  
*(xend, yend)* -- co-ordinates of the end point of the fracture (m)  
*kode* – no function  
*jmat* -- joint property ID defined before (*jmat=1,2,3 ...* )

**ARCH** define an arch or a tunnel/borehole

***num, xcen, ycen, diam, ang1, ang2, kode, bvs, bvsn***

*num* -- number of elements on arch boundary  
*(xcen, ycen)* -- coordinates of arch centre (m)  
*diam* -- arch diameter (m)  
*ang1* -- beginning angle of the arch (clockwise) (degree)  
*ang2* – end angle of the arch (clockwise) (degree)  
*kode* -- type of boundary condition  
 = 1, shear and normal stress boundary

- = 2, shear and normal displacement boundary
- = 3, shear displacement and normal stress boundary
- = 4, shear stress and normal displacement boundary
- bvs* -- boundary value in shear direction (stress or displacement) (Pa or m)
- bvn* -- boundary value in normal direction (stress or displacement) (Pa or m)

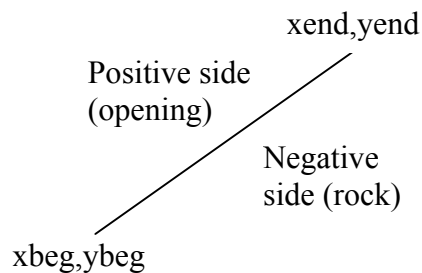
**Warning:** For an excavation opening, the arch angle starts from low to high (e.g. 0°–180°). For a solid disc the arch angle starts from high to low (e.g. 180°–0°).

**EDGE** define a straight boundary line

*num, xbeg, ybeg, xend, yend, kode, bvs, bvn*

- num* -- number of elements along the edge
- (xbeg,ybeg)* -- co-ordinates of the beginning point of the edge (m)
- (xend,yend)* -- co-ordinates of the end point of the edge (m)
- kode* -- type of boundary condition
  - = 1, shear and normal stress boundary
  - = 2, shear and normal displacement boundary
  - = 3, shear displacement and normal stress boundary
  - = 4, shear stress and normal displacement boundary
- bvs* -- boundary value in shear direction (stress or displacement) (Pa or m)
- bvn* -- boundary value in normal direction (stress or displacement) (Pa or m)

**Warning:** The beginning point and the end point need to be defined in a sequence that the positive side of the edge is always the excavation. The positive side and the negative side are defined as:



**CYCL** *cnum* start calculation

*cnum* – number of cycle to be performed (one cycle often produces one step of crack growth for each unstable crack tip). If *cnum* is not given, the default cycle number is 1000.

**SAVE** *filename* save the current state of calculation into a file

Note: the saved state of modelling can be restarted later using Window commands.

**STOP** Stop the calculation

***QUIT*** Stop the calculation

***ENDF*** End of the input data file

To help preparing the input file, an input pre-processor (***Model Design***) has been developed for the user's convenience. The interface is fully Window based and is coupled with graphics to help in defining a model easily. An instruction of how to use ***Model Design*** is described in Appendix I.

## 5 CONDUCT AND MONITOR THE CALCULATION

The FRACOD code is created as an executable file (Fracod2D.exe). To start the code FRACOD, simply double-click the executable file in Windows, a dialog menu will appear on your screen. You then need to open an input data file or a FRACOD save file, by using the open file options. If you are starting a new problem, you need to load a input data file which has already been prepared either by using a text editor or by using the model design function provided in the code (see Appendix I). If you are restarting a problem which has previously been run and saved, you then need to load the saved file (\*.sav). FRACOD will automatically detect whether the file you are loading is an input data file or a save file. Once a calculation has started, it will continue until it is interrupted manually, or the defined cycles finished, or no more fracture propagation is found. During the calculation, the instant geometry of the modelled fracture network is always shown on the screen so that any growth of the fractures can be monitored. The fractures are plotted in different colours to distinguish whether the fracture surfaces are in elastic contact, open or sliding (the colours can be specified or changed by users). When a calculation is completed or is interrupted, a number of screen commands are available to plot the stress/displacement or to change the parameters etc. These commands are provided as icons on the program window and can be easily activated by clicking the mouse. The key functions of the available screen commands are shown below.

**File (Load, Save, Print, Exit)*****Load***

Load an input data file (\*.dat) or a saved file (\*.sav)

**Input File (\*.dat)**

Load an input data file and start a new problem which is defined in the input data file. An input data file is a text file that contains commands and values to define a problem. This is a file being prepared in advance by the user using any text editor following the format that FRACOD can recognise, or using the pre-processing functions (Appendix I) provided with the FRACOD code.

**Saved File (\*.sav)**

Load a saved file and continue the simulation which was previously interrupted. A saved file is a file containing data of a problem run previously by using FRACOD. The data in the file is computer coded and can only be read by FRACOD itself. An ongoing fracture propagation modelling can be interrupted (see **Pause**) and saved (see **Save**) into a saved file. The saved file can then be reloaded into FRACOD to continue the previously interrupted modelling.

**Movie File (\*.mvi)**

Load a movie file to replay the progress of fracture propagation from previous calculations. A movie file is a file containing plot data of a problem run previously by using FRACOD. It is saved automatically during FRACOD calculation using the same name as the input data file but with the extension of “.mvi”. This function provides the possibility of replaying/printing the fracture propagation process without re-running the model.

***Save (Run, Plot)*****Run**

Save the current status of calculation into a saved file. The saved file can later be reloaded (see **Load**) into FRACOD to continue the modelling.

**Plot**

Save the current plot into a file (\*.emf, or \*.wmf). The file has a emf (Window Meta Files) or wmf (Window Enhanced Meta Files) format. It can be copied to other Window applications (e.g. MS Word).

***Print***

Print the current screen plot on a default output device (printer).

***Exit***

Terminate the current calculation and close the FRACOD Window.

***Default screen output***

During simulation, the geometry of fractures and tunnels etc. will be automatically shown on the screen. The picture will be updated after each calculation cycle to trace any fracture propagation. In this way the whole process of fracture propagation can be monitored. In the screen plot, fractures are plotted with different colours to show the state of the fractures, i.e. elastic contact, sliding or open. The default fracture colour is:

- Blue – elastic fracture
- Green – sliding fracture
- Red – open fracture.

The colour can be changed by users in *view/plots setup*.

The magnitudes of far-field stresses are shown in the *Legend* plot window. Here:

- Pxx – normal stress in the horizontal direction of the model
- Pyy – normal stress in the vertical direction of the model
- Pxy – shear stress

The magnitudes of stresses are in Pa unless specified otherwise.

***Edit (Copy to Clipboard (BMP), Copy to ClipBoard (EMF))***

Copy the screen plot to the clipboard in the BitMap Format (BMP) or in Window Enhance Meta Files format (EMF). The plot can be pasted to other Window applications (e.g. MS Word).

***View (Model Geometry, Principal Stress, Max. Shear Stress, Displacement)***

Plot the stresses or displacements from a paused simulation on screen. An ongoing simulation can be paused (see ***Pause***) and the geometry, stresses and displacements can be plotted on screen.

***Geometry***

Plot on screen the geometry of the fractures and other boundaries such as tunnels in the model. The geometry plot is set as default and is automatically shown on the screen during calculation.

***Principal Stress***

Plot on screen the principal stresses in the rock mass within a defined window. Two orthogonal principal stresses, the major principal stress and the minor principal stress, will be plotted on screen as two orthogonally lines. The directions of the lines are the directions of the two principal stresses, and the length of each line is proportional to the stress magnitude. Colours are used to distinguish the compressive stress with the tensile stress:

- Blue – compressive stress (default)
- Red – tensile stress (default)

The colour can be changed by user in ***View/Plot setup***.

The maximum magnitude of the principal stresses in the plot is given in the ***Legend*** window (in Pa)

***Max. Shear Stress***

Plot on screen the maximum shear stress in the rock mass within a defined window. The maximum shear stress in two orthogonal directions will be plotted on the screen as two orthogonal lines. The directions of the lines are the directions of the maximum shear stress, and the length of each line is proportional to the stress magnitude.

The maximum magnitude of the maximum shear stresses in the plot is given in the ***Legend*** window (in Pa)

***Displacement***

Plot on screen the displacement vector at specified grid points in the model. Rock displacement at a grid point will be plotted on the screen as a vector with an arrow indicating the direction of the displacement, and the length of the vector is proportional to the values of displacement.

The value of maximum displacement in the plot is given on the top of the plot window (in metres).

***View (Image, Legend)***

***Image (currently not functional)***

Plot on screen the filled contours of stresses or displacement.

***Legend***

Show the legend on the plot window. Included in the Legend are:

- Far-field stress ( $S_{xx}, S_{yy}, S_{xy}$ )
- Maximum values of the stresses or displacement appeared on the screen plot.
- Colour conventions

***View (Zoom in, Zoom out, Full plot)***

***Zoom in***

Enlarge the plot in a specified window (defined by dragging the *Mouse*).

***Zoom out***

Reduce the plot the plot in a specified window (defined by dragging the *Mouse*).

***Full screen***

Return the plot size to the originally specified window (full screen).

***View (Magnifier, Plot setup)***

***Magnifier***

Magnify an area of the screen. To do so, locate the mouse cursor to the desired position and press down the mouse right button.

***Plot setup***

Specify or change the plot setup, including:

- Line colour
- Line thickness
- Plot range
- Problem title
- Axis setting

***Run (Run, Pause, Stop)***

***Run***

Start or continue a calculation. A cycle number is requested. One cycle often produces a fracture propagation of one element length.

***Pause***

Pause the current calculation. A paused calculation can be reactivated and continued by using ***Run***.

***Stop***

Stop the calculation. This command triggers the termination of the current calculation. A stopped calculation cannot be restarted. Some calculation results (stresses and displacement at the previously specified grid points) can, however, still be shown.

**Option (*Far-field stress, Boundary stress*)**

Change the magnitude of the far-field stresses or boundary stresses

***Far-field stress***

Increase or decrease the magnitude of far-field stresses. The value of increment or reduction is requested. Note that the compressive stress is negative, so that an increment in compressive stress should be given as a negative values.

This command is particularly useful in studying the change of the fracture growth path when the far field stresses are changed.

***Boundary stress***

Increase or decrease the magnitude of boundary stresses (or displacement if the boundary condition is specified by displacement). The value of increment or reduction of shear or normal stress is requested. Note that the compressive stress is negative, so that an increment in compressive stress should be given as a negative value.

This command is particularly useful in studying the change of the fracture growth path when the boundary stresses (e.g. hydraulic pressure in a borehole) are changed.

***Tools (Model design)***

A pre-processor which helps the user to set up the numerical model. Details of the pre-processor are given in Appendix I.

***Windows (...)***

Standard Window management functions which enable users to arrange the multiple calculation Windows.

***Help (...)***

On-line user's manual and helping functions.

## REFERENCES

- Crouch S.L., 1976.** Solution of plane elasticity problems by the displacement discontinuity method. *Int. J. Num. Methods Engng.* **10**, 301-343.
- Crouch S.L. and Starfield A.M., 1983.** *Boundary element methods in solid mechanics.* George Allen & Unwin (publisher).
- Eordgan F. and Sih G.C., 1963.** On the crack extension in plates under plane loading and transverse shear. *ASME J. Bas. Engng* **85**, 519-527.
- Griffith, A., 1921.** The phenomena and rupture flow in solids. *Phil. Trans. R. Soc. London.* **A221**, 163-198.
- Griffith, A., 1925.** The theory of rupture. *Proc. 1st Int. Cong. Appl. Mech., Delft.* 55-63.
- Hellan K., 1985.** *Introduction to fracture mechanics.* McGraw-Hill Book Company (publisher).
- Hoori H. and Nemat-Nasser S., 1985.** Compression-induced microcrack growth in brittle solid: axial splitting and shear failure. *J. Geophy. Res.* **90**(B4), 3105-3125.
- Horri H. and Nemat-Nasser S., 1986.** Brittle failure in compression: splitting, faulting and brittle-ductile transition. *Phil. Trans. Roy. Soc.,* **319** (1549), 337-374.
- Hussain M.A., Pu S.L. and Underwood J., 1974.** Strain energy release rate for a crack under combined mode I and mode II. *Fracture Analysis, ASTM-STP.* **560**, 2-28. Am. Soc. Testing Materials, Philadelphia.
- Ingrafea A., 1987.** Finite element models for rock fracture mechanics. *Int. J. Num. Ana. Meth. Geomech.* **4**, 24-43.
- Kachanov, M.L., 1982.** A microcrack model of rock inelasticity —Part I and II. *Mech. Mater.* **1**, 19-41.
- Kemeny, J.M. and Cook, N.G.W., 1991.** Micromechanics of deformation in rocks. In: *Toughening Mechanisms in Quasi-Brittle Materials*, S.P. Shaw (ed). Kluwer Academic, The Netherland, 155-188.

- Kemeny, J.M., 1991.** A model for non-linear rock deformation under compression due to subcritical crack growth. *Int. J. Rock Mech. Min. Sci.* **28**, 459-467.
- Lajtai E.Z., 1969.** Shear strength of weakness planes in rock. *Int. J. Rock Mech. Min. Sci. & Geomech. Abs.* **6**, 299-515.
- Lajtai E., 1974.** Brittle fracture in compression. *Int. J. Fracture*, **10**(4), 525-536.
- Li V.C., 1991.** Mechanics of shear rupture applied to earthquake zones. In: *Fracture mechanics of rock*, Atkinson K.B. (ed). Academic Press, London, 351-428.
- Lockner D., Moore D. and Reches Z., 1992.** Microcrack interaction leading to shear fracture. *Proc. 33rd U.S. Symp. Rock Mech.* 807-816.
- Melin S., 1985.** The infinitesimal kink. Report LUTFD2/(TFHF-3022)/1-19/(1985). (Division of Solid Mechanics, Lund Institute of Technology, Lund.)
- Petit J.-P. and Barquins M., 1988.** Can natural faults propagate under mode II conditions? *Tectonics*, **7**(6), 1243-1256.
- Reyes O. and Einstein H.H., 1991.** Failure mechanism of fractured rock — A fracture coalescence model. *Proc. 7th Int. Con. on Rock Mechanics*, **1**, 333-340.
- Rao Q., 1999.** Pure shear fracture of brittle rock – A theoretical and laboratory study. PhD Thesis 1999:08, Lulea University of Technology.
- Savilahti T., Nordlund E. and Stephansson O., 1990.** Shear box testing and modelling of joint bridges. In: *Rock Joints*, Barton & Stephansson (eds). *Proc. Int. Symp. Rock Joints (Norway)*. 295-300.
- Schultz R., 1988.** Stress intensity factors for curved cracks obtained with the displacement discontinuity method. *Int. J. Fracture*, **37**, R31-34.
- Segall P. and Pollard D., 1980.** Mechanics of discontinuous faults. *J. Geophys. Res.* **85**(B8), 4337-4350.
- Segall P. and Pollard D., 1983.** Nucleation and growth of strike slip faults in granite. *J. Geophys. Res.* **88**(B1), 555-568.
- Shen B. and Stephansson O., 1992.** Deformation and propagation of finite joints in rock masses. In: *Myer et al. (eds): Fractured and Jointed Rock Masses*. 303-309.

**Shen B. and Stephansson O., 1993.** Numerical analysis of Mode I and Mode II propagation of rock fractures. *Int. J. Rock Mech. Min. Sci. & Geomech. Abst.* **30(7)**, 861-867.

**Shen B. and Stephansson O., 1993.** Modification of the G-criterion of crack propagation in compression. *Int. J. of Engineering Fracture Mechanics.* **47(2)**, 177-189.

**Shen B., Stephansson O., Einstein H.H. and Ghahreman, B., 1995.** Coalescence of fractures under shear stresses in experiments. *J. Geophys. Res.* **100(B4)**, 5975-5990.

**Shen, B., 1995.** The mechanism of fracture coalescence in compression - experimental study and numerical simulation. *Int. J. of Engineering Fracture Mechanics.* **51(1)**, 73-85.

**Shen B., Tan, X. Li C. and Stephansson O., 1997.** Simulation of borehole breakout using fracture mechanics models. *In: Rock Stress, Sugawara & Obara (eds). Balkema, Rotterdam.* 289-298.

**Shen B. and Rinne M., 2001.** Generalised criteria for fracture initiation at boundaries or crack tips. Report prepared for SKB.

**Sih G.C., 1974.** Strain-energy-density factor applied to mixed mode crack problems. *Int. J. Fracture.* **10(3)**, 305-321.

**Wang R., Zhao Y., Chen Y., Yan H., Yin Y., Yao C. and Zhang H., 1987.** Experimental and finite element simulation of X-type shear fractures from a crack in marble. *Tectonophysics.* **144**, 141-150.

**Wong, T-F, 1982.** Micromechanics of faulting in Westerly granite. *Int. J. Rock Mech. Min. Sci.* **19**, 49-64.

## **ACKNOWLEDGEMENTS**

This work is financially supported by Fracom Ltd, Tekes and SKB. The current FRACOD code is based on the original version developed under the supervision of Professor Ove Stephansson of KTH. The author wishes to thank Professor Stephansson for his invaluable input in the code, particularly in the early stages of development. The author would also like to thank Mr. Mikael Rinne for his collaboration in the code development and his careful checking of the code, Dr. Kennert Röshoff for his initiation and coordination of the study. Valuable comments from Mr. Christer Svemar, Mr. Rolf Christiansson and Prof. John Cosgrove are gratefully acknowledged.

## APPENDIX I – HOW TO USE THE PREPROCESSOR TO SET UP MODELS

FRACOD provides a pre-processor to help users in setting up the numerical model. The pre-processor is a Window based interface which enables users to see instantly the geometry of the fractures and boundaries they have defined. It also provides pop-up windows to guide the input whenever values are needed. After all the fractures and parameters are defined for a problem, a FRACOD input data file can then be created in a format that FRACOD can read and it is equivalent to the data file created manually by using a text editor.

The pre-processor can be activated by clicking *Model Design* in the *display* Window (i.e. the default Window when FRACOD is activated). A second Window, i.e. the *Model Design* Window will then pop up. The following key functions are included in the *Model Design* Window.

### *File (Load, SaveAs, Print)*

#### *Load*

Open an existing FRACOD input data file. The model geometry and mechanical properties defined by the file will be loaded into the memory and can be shown on the screen. They can also be modified by the user.

#### *SaveAs*

Save the defined model into a FRACOD input data file.

#### *Print*

Print the current model geometry.

### *Edit (Copy to Clipborad (BMP); Copy to Clipborad (EMF))*

#### *Copy to Clipborad (BMP)*

Copy the current model geometry to Clipborad in BitMap format. It can later be pasted to other Window applications (such as MS Word).

### ***Copy to Clipboard (EMF)***

Copy the current model geometry to Clipboard in Enhanced Window Meta Format. It can later be pasted to other Window applications (such as MS Word).

### ***View (Model Properties)***

#### ***Model Properties***

View the properties of a selected object (fracture, edge, arc etc.). The geometrical properties will be shown immediately after this function is selected.

If the selected object is a fracture, the mechanical properties (shear and normal stiffness, friction angle and cohesion) can be viewed and modified by clicking icon “*Define Fracture Properties*” in the current Window.

If the selected object is a boundary (edge, hole etc.), the boundary conditions of the object can be viewed and modified by clicking icon “*Define Boundary Conditions*”.

### ***SetUp (Set Parameters)***

#### ***Set Parameters***

Set up the model geometrical and mechanical parameters. Options include:

Caption: Give a title to the current model.

Symmetry: Define the symmetry condition of the model.

XY Range: Define the range of display for both Model Design and the fracture propagation modelling

Properties: Define the mechanical properties of intact rock (Young's modulus, Poisson's ratio, critical strain energy release rates  $G_{Ic}$  and  $G_{IIc}$ ) and fractures (shear and normal stiffness, friction angle, cohesion). Up to 10 different fracture properties can be given, each with a material index number (=1-10). Different fractures can be assigned with different fracture properties. Also should be given here are the far-field stresses applied in the model. Intact rock properties for fracture initiation.

## Shapes

This is an interactive function allowing users to define the model geometry such as boundaries and fractures. It includes the following options:

### Arc-Disc (in: *Shapes/Arc/Arc-Disc*)

Define a disc or part of a disc. The geometrical properties as well as the boundary conditions can be defined and altered in **View (Object Properties)**. The disc can also be repositioned and resized by selecting and dragging the object using mouse.

A disc is defined by giving the coordinate of the centre point, the diameter and the start and end angles (default  $180^\circ$  to  $-180^\circ$ ). The start and end angles have to be defined in clockwise.

### Arc-Hole (in: *Shapes/Arc/Arc-Hole*)

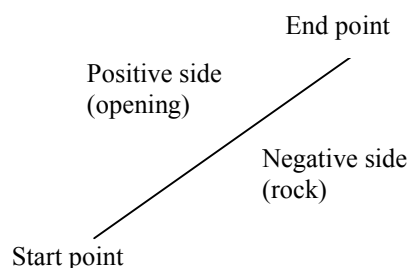
Define a hole (tunnel) in a rock mass. The geometrical properties as well as the boundary conditions can be defined and altered in **View (Object Properties)**. The hole can also be repositioned and resized by selecting and dragging the object using mouse.

A hole is defined by giving the coordinate of the centre point, the diameter and the start and end angles (default  $-180^\circ$  to  $180^\circ$ ). The start and end angles have to be defined in anti-clockwise.

### Edge (in: *Shapes/Line/Edge*)

Define an edge (i.e. a straight boundary) in a rock mass. The geometrical properties as well as the boundary conditions can be defined and altered in **View (Object Properties)**. The edge can also be repositioned and resized by selecting and dragging the object using mouse.

An edge is defined by giving the coordinates of the start and end points. The start and end points have to be arranged in such a way that the negative side of the edge is the rock mass, as shown below.



### Fracture (in: *Shapes/Line/Fracture*)

Define a fracture in a rock mass. The geometrical properties as well as the mechanical properties of the fracture can be defined and altered in ***View (Object Properties)***. The fracture can also be repositioned and resized by selecting and dragging the object using mouse.

A fracture is defined by giving the coordinates of the start and end points. The definition of a fracture is not sensitive to the sequence of the start and end points.

## APPENDIX II – VERIFICATION AND APPLICATION OF FRACOD

Eleven demonstration problems are listed here as part of the verification and application tests of the FRACOD code. The data files are provided in the program package.

### Example 1 – Single fracture subjected to normal tensile stress

#### (1) Problem definition

A 2m fracture in an infinite rock mass is under uniaxial tensile stress of 50MPa in the direction perpendicular to the fracture plane. The elastic properties of the rock mass are:

$$E = 40GPa$$

$$\nu = 0.25.$$

The strain energy release rate in mode I for this problem is calculated by using the FRACOD code with 30 elements along the fracture.

$$(G_I)_{FRACOD} = 190 \times 10^3 J/m^2$$

The theoretical solution of this problem gives the stress intensity factor ( $K_I$ ) as

$$K_I = \sigma \sqrt{\pi a}$$

$$= 50 \times \sqrt{3.1416 \times 1} = 88.6 MPa \sqrt{m}$$

where a = half length of the fracture.

The theoretical strain energy release rate is then calculated as:

$$(G_I)_{theory} = \frac{1-\nu^2}{E} (K_I)^2$$

$$= \frac{1-0.25^2}{40 \times 10^9} \times (88.6 \times 10^6)^2 = 184 \times 10^3 J/m^2$$

The difference between the numerical result and the theoretical result is approximately 3%.

In this example, the critical strain energy release rates of fracture propagation are:

$$G_{Ic} = 50 \text{ J/m}^2$$

$$G_{IIc} = 1000 \text{ J/m}^2 .$$

As the fracture propagation is pure mode I along the fracture's original plane, only the critical strain energy release rate in mode I ( $G_{Ic}$ ) is useful. The F-value obtained from the FRACOD modelling is:

$$F(0) = \frac{G_I(0)}{G_{Ic}} + \frac{G_{II}(0)}{G_{IIc}}$$

$$= \frac{190 \times 10^3}{50} + \frac{0}{1000} = 3800$$

The F-value is by far greater than the critical value 1.0. Hence fracture propagation is detected.

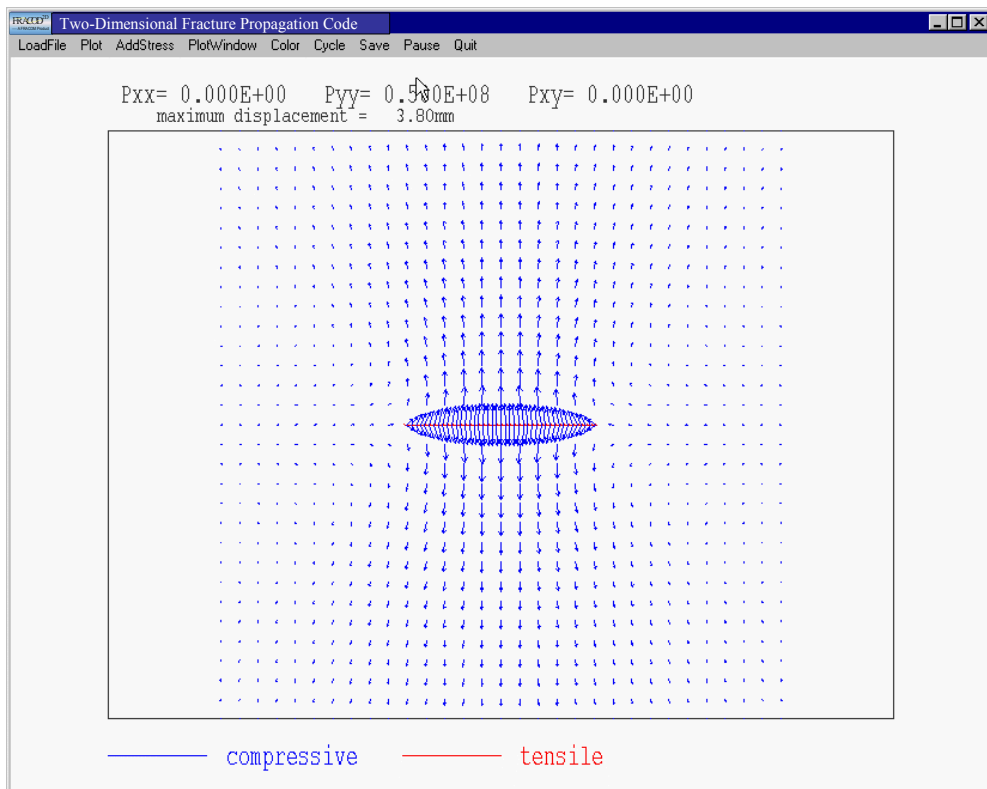
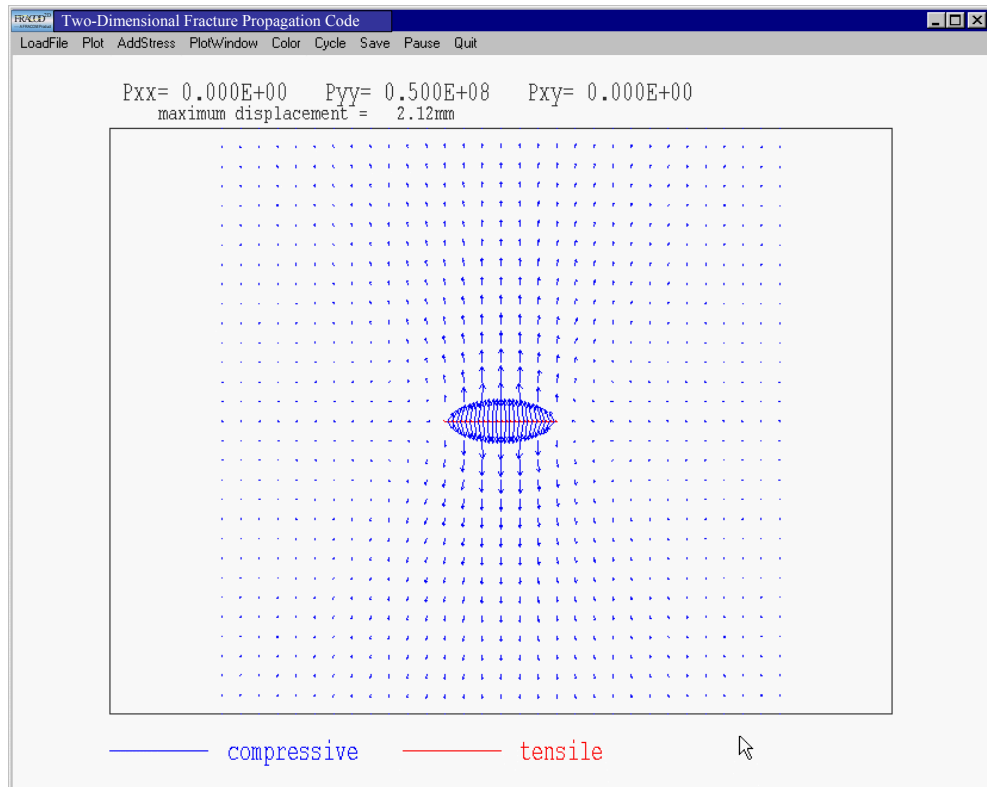
(2) *Input data*

```

-----
TITLE
Single fracture subjected to normal tensile stress
SYMMETRY -- Model symmetry
  0 0.00 0.00
MODULUS -- Poisson's Ratio and Young's modulus
  0.25 0.40E+11
TOUGHNESS -- Gic and Giic
  50. 1000.
PROPERIES -- mat, kn, ks,phi,coh
  1 0.10E+14 0.10E+14 30.0 0.00E+00
SWINDOW -- xll,xur,yll,yur,numx,numy
  -3.00 3.00 -3.00 3.00 30 30
STRESSES -- sxx,syy,sxy
  -0.0E+07 0.50E+08 0.00E+00
FRACTURE -- nume,xbeg,ybeg,xend,yend,kode,mat
  30 -1.000 -0.000 1.000 0.000 2 1
CYCL 1000
ENDFILE
-----

```

(3) *FRACOD model*



**Example 2 – Single fracture subjected to pure shear stress**

(1) *Problem definition*

A 2m fracture in an infinite rock mass is under pure shear stress of 50MPa. The elastic properties of the rock mass are the same as in Example 1.

According to Rao (1999), a fracture in pure shear may propagate in mode I or mode II depending on the ratio of the fracture toughness of mode I and mode II ( $K_{Ic}/K_{IIc}$ ). Only when  $K_{Ic}/K_{IIc} > 1.15$ , a mode II fracture propagation can occur. The FRACOD code is used in this example to compare with the theoretical results.

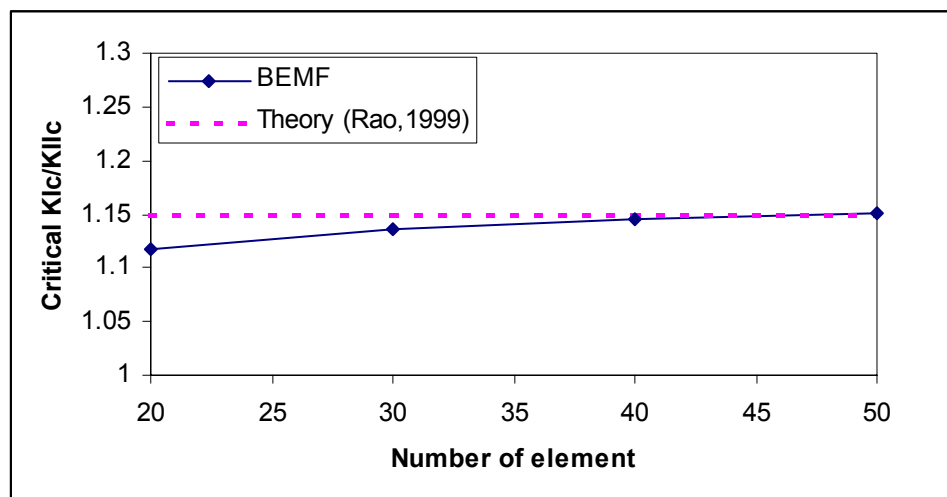
30 elements are used along the fracture. The critical mode II strain energy release rate ( $G_{IIc}$ ) is taken as 1000 J/m<sup>2</sup>. The critical mode I strain energy release rate ( $G_{Ic}$ ) is varied to obtain the critical ratio ( $G_{Ic}/G_{IIc}$ ) at which the fracture propagation starts to change mode. It was found that  $G_{Ic} = 1289$  J/m<sup>2</sup> is the critical value for the fracture propagation to change mode. When  $G_{Ic} < 1289$  J/m<sup>2</sup>, the fracture propagates in mode I in the direction of about 70° from the original fracture plane; when  $G_{Ic} > 1289$  J/m<sup>2</sup>, the fracture starts to propagate in mode II in its own plane, see Figures.

Use the relation between the critical stress energy release rate and the fracture toughness

$$\left( \frac{K_{Ic}}{K_{IIc}} \right)_{numerical} = \sqrt{\frac{G_{Ic}}{G_{IIc}}} = \sqrt{\frac{1289}{1000}} = 1.135.$$

The critical toughness ratio for mode II fracture propagation obtained numerically by using the FRACOD code is 1.135, very close to the analytical solution of 1.15 reported by Rao (1999).

Using different number of elements along the fracture, the comparison between the FRACOD results and the theoretical results is shown in the figure below.



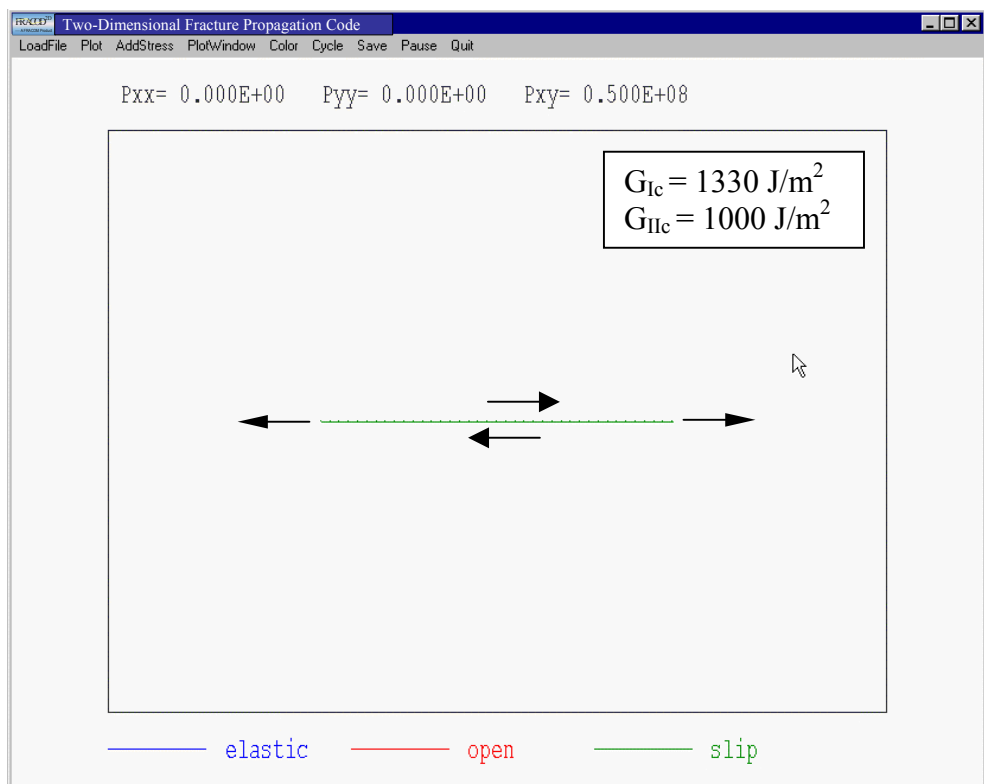
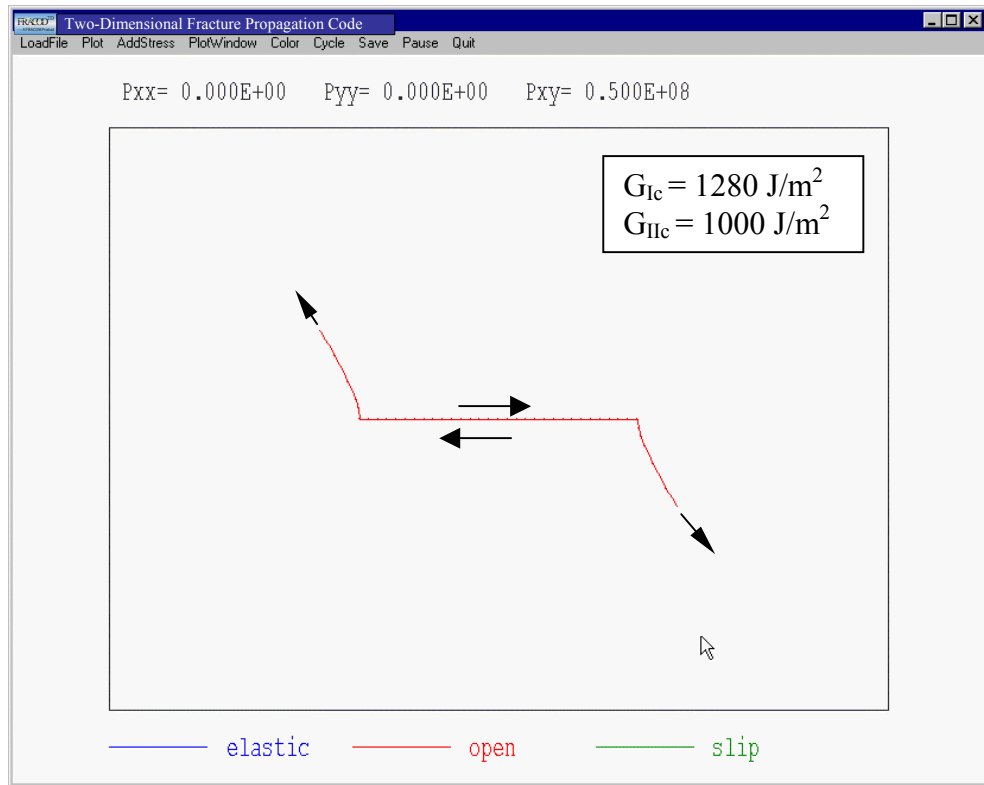
(2) *Input data*

```

-----
TITLE
Single fracture subjected to pure shear stress
SYMMETRY -- Model symmetry
  0 0.00 0.00
MODULUS -- Poisson's Ratio and Young's modulus
  0.25 0.40E+11
TOUGHNESS -- Gic and Giic
  1289.0 1000.
PROPERIES -- mat, kn, ks,phi,coh
  1 0.0E+0 0.0E+0 0.0 0.00E+00
SWINDOW -- xll,xur,yll,yur,numx,numy
  -2.00 2.00 -2.00 2.00 30 30
STRESSES -- sxx,syy,sxy
  -0.0E+06 -0.00E+0 50.00E+06
FRACTURE -- nume,xbeg,ybeg,xend,yend,kode,mat
  30 -1. 0. 1. 0. 2 1
CYCL 1000
ENDFILE
-----

```

(3) *FRACOD model*



**Example 3 – Single inclined fracture subjected to uniaxial compression***(1) Problem definition*

An inclined fracture in an infinite rock mass is under uniaxial compressive stress of 50MPa. The inclination of the fracture is 45°. The elastic properties of the rock mass and the fracture critical strain energy release rates are the same as in Example 1. The contact properties of the fracture surfaces are:

$$\begin{aligned}K_n &= 1000\text{GPa/m} \\K_s &= 1000\text{GPa/m} \\ \phi &= 30^\circ \\ c &= 0\end{aligned}$$

The fracture is found to propagate in mode I in the direction nearly parallel to the far-field stress.

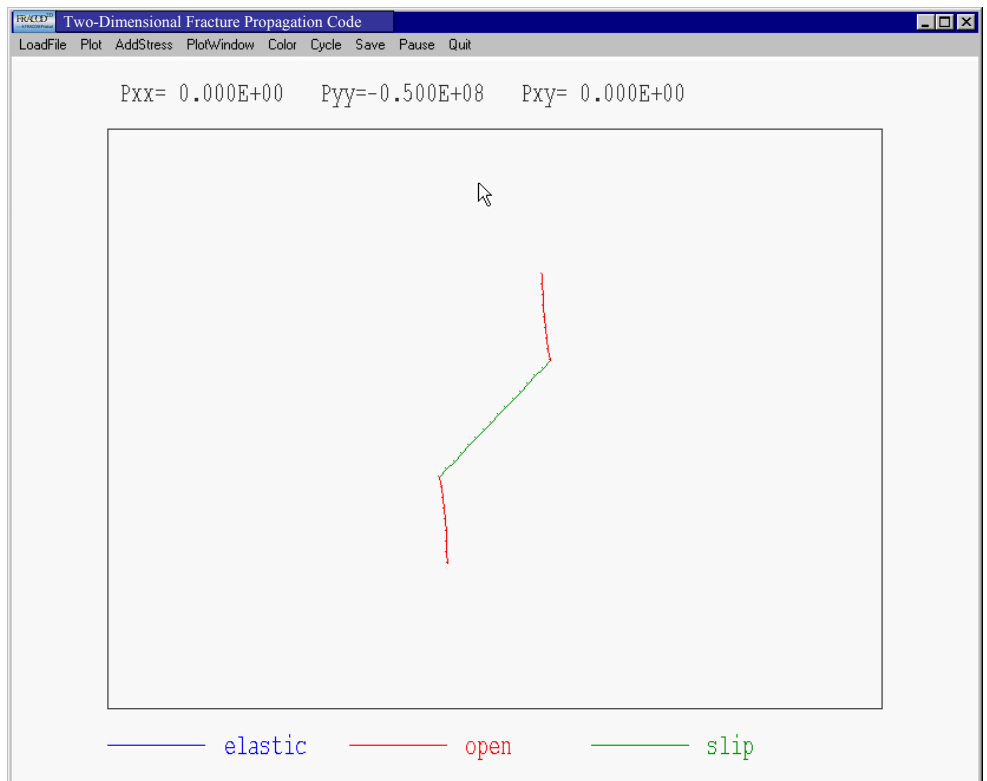
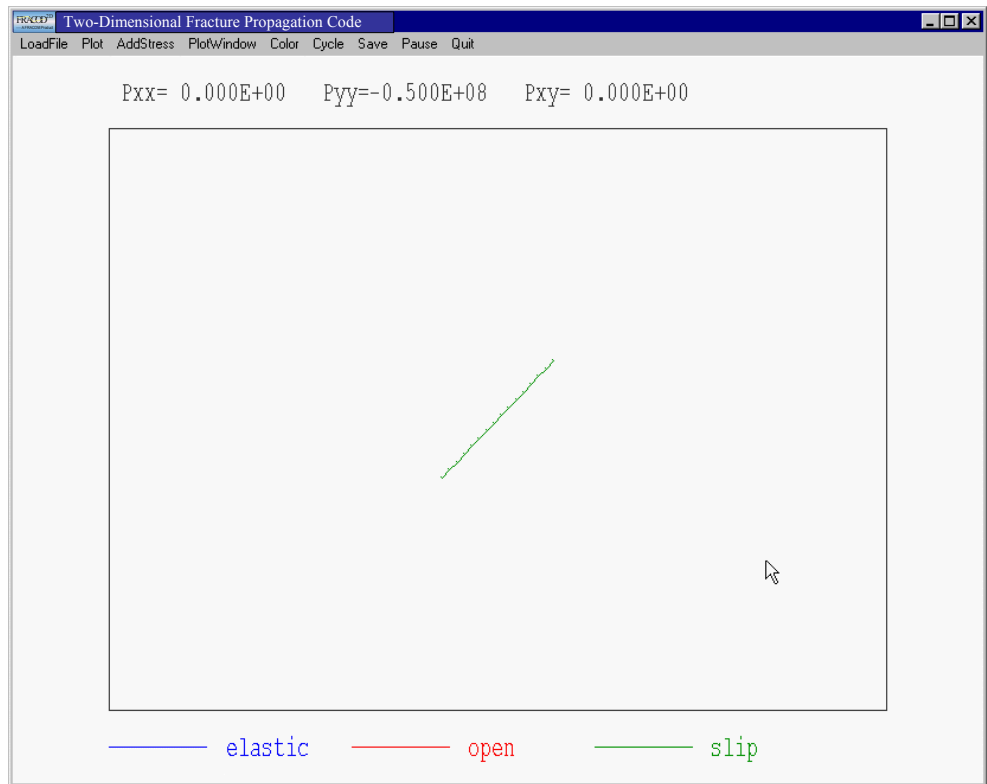
*(2) Input data*

```

-----
TITLE
Single inclined fracture subjected to uniaxial compression
SYMMETRY -- Model symmetry
  0 0.00 0.00
MODULUS – Poisson's Ratio and Young's modulus
0.25 0.40E+11
TOUGHNESS -- Gic and Giic
50. 1000.
PROPERIES -- mat, kn, ks,phi,coh
  1 0.10E+13 0.10E+13 30.0 0.00E+00
SWINDOW -- xll,xur,yll,yur,numx,numy
-5.00 5.00 -5.00 5.00 30 30
STRESSES -- sxx,syy,sxy
-0.0E+07 -0.50E+08 0.00E+00
FRACTURE -- nume,xbeg,ybeg,xend,yend,kode,mat
 15 -1.000 -1.000 1.000 1.000 2 1
CYCL 1000
ENDFILE
-----

```

(3) *FRACOD model*



**Example 4 – Single inclined fracture subjected to biaxial compression***(1) Problem definition*

An inclined fracture in an infinite rock mass is subjected to compressive loading stress of 50MPa and confining stress of 10MPa. The inclination of the fracture is 45°. The material properties of the rock mass and fractures are the same as in Examples 1 and 3.

The fracture is found to propagate mainly in mode II in the direction about 60° to the confining stress.

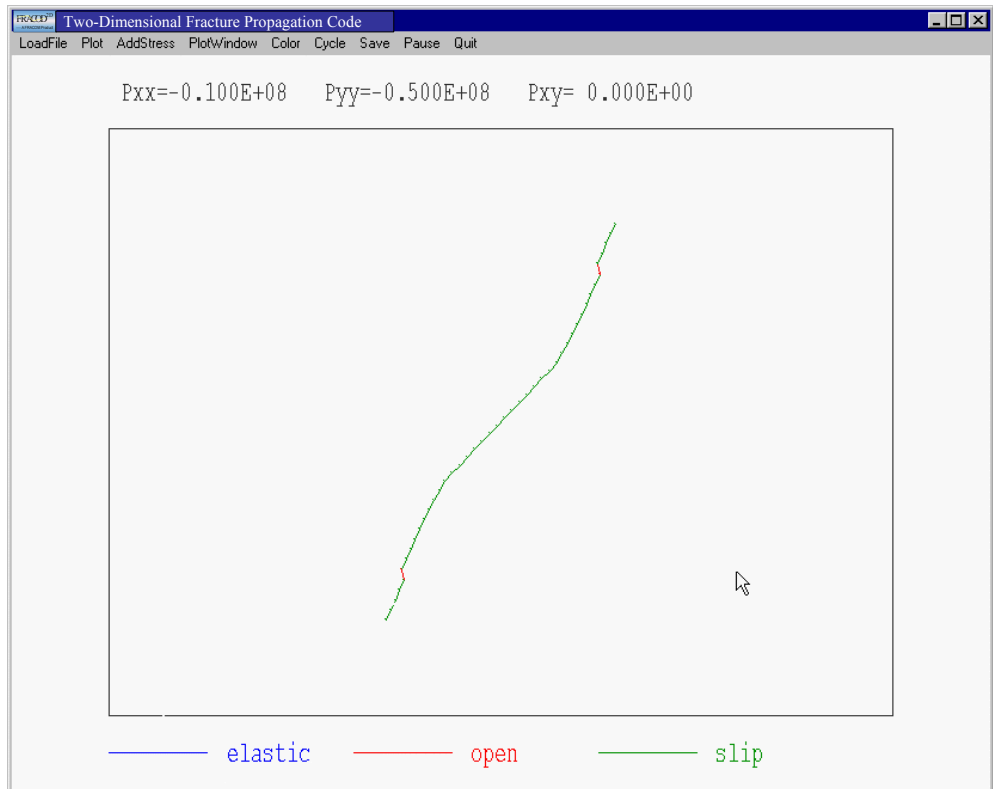
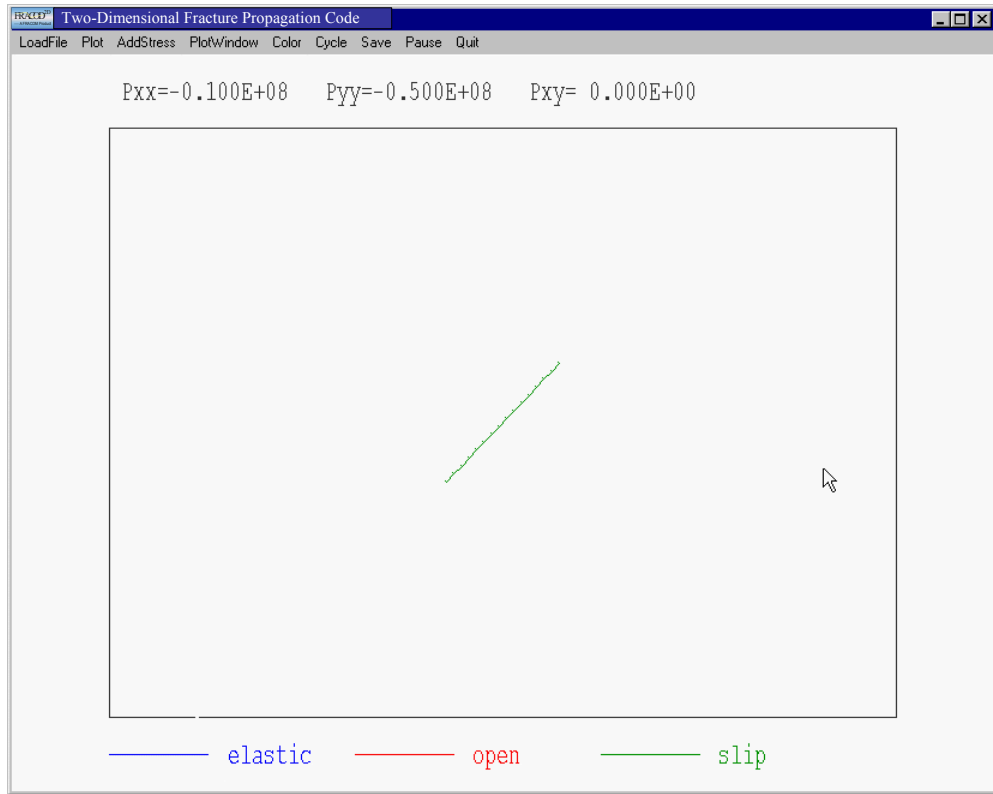
*(2) Input data*

```

-----
TITLE
Single inclined fracture subjected to biaxial compression
SYMMETRY -- Model symmetry
  0 0.00 0.00
MODULUS – Poisson's Ratio and Young's modulus
  0.25 0.40E+11
TOUGHNESS -- Gic and Giic
  50. 1000.
PROPERIES -- mat, kn, ks,phi,coh
  1 0.10E+13 0.10E+13 30.0 0.00E+00
SWINDOW -- xll,xur,yll,yur,numx,numy
  -5.00 5.00 -5.00 5.00 30 30
STRESSES -- sxx,syy,sxy
  -0.10E+08 -0.50E+08 0.00E+00
FRACTURE -- nume,xbeg,ybeg,xend,yend,kode,mat
  15 -1.000 -1.000 1.000 1.000 2 1
CYCL 1000
ENDFILE
-----

```

(3) *FRACOD model*



**Example 5 – Single inclined fracture subjected to biaxial compression***(1) Problem definition*

An inclined fracture in an infinite rock mass is subjected to compressive stress of 50MPa and confining stress of 7.5MPa. The inclination of the fracture is 45°. The material properties of the rock mass and fractures are the same as in Examples 1 and 3.

The fracture is found to propagate in mixed mode I and II in the overall direction about 70° to the confining stress.

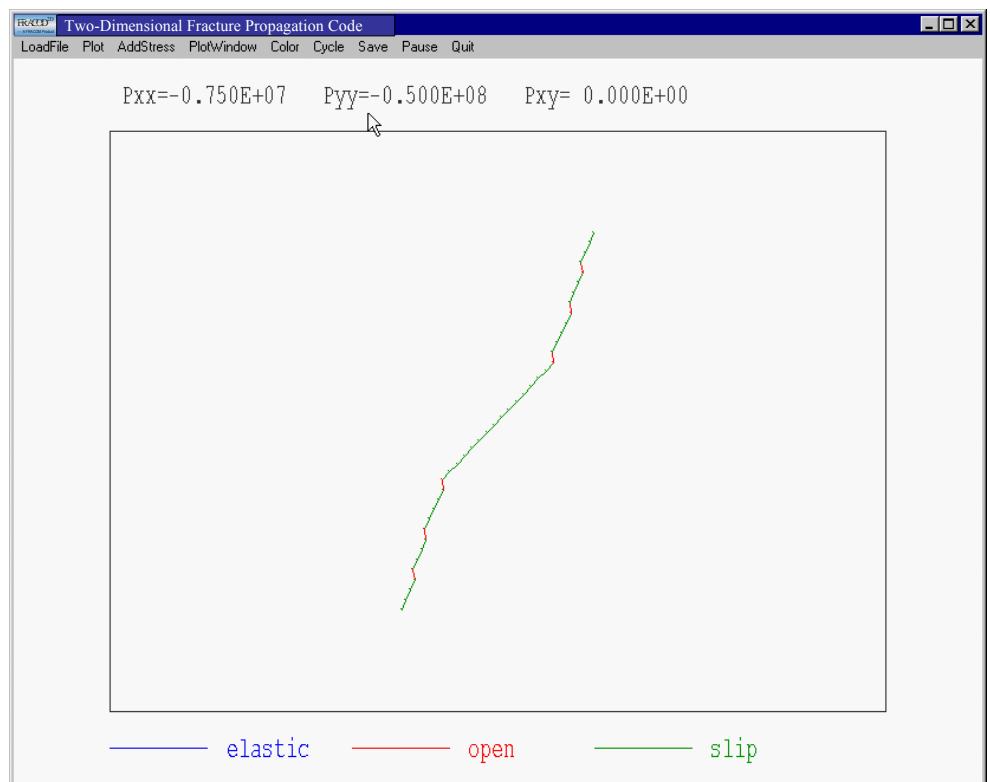
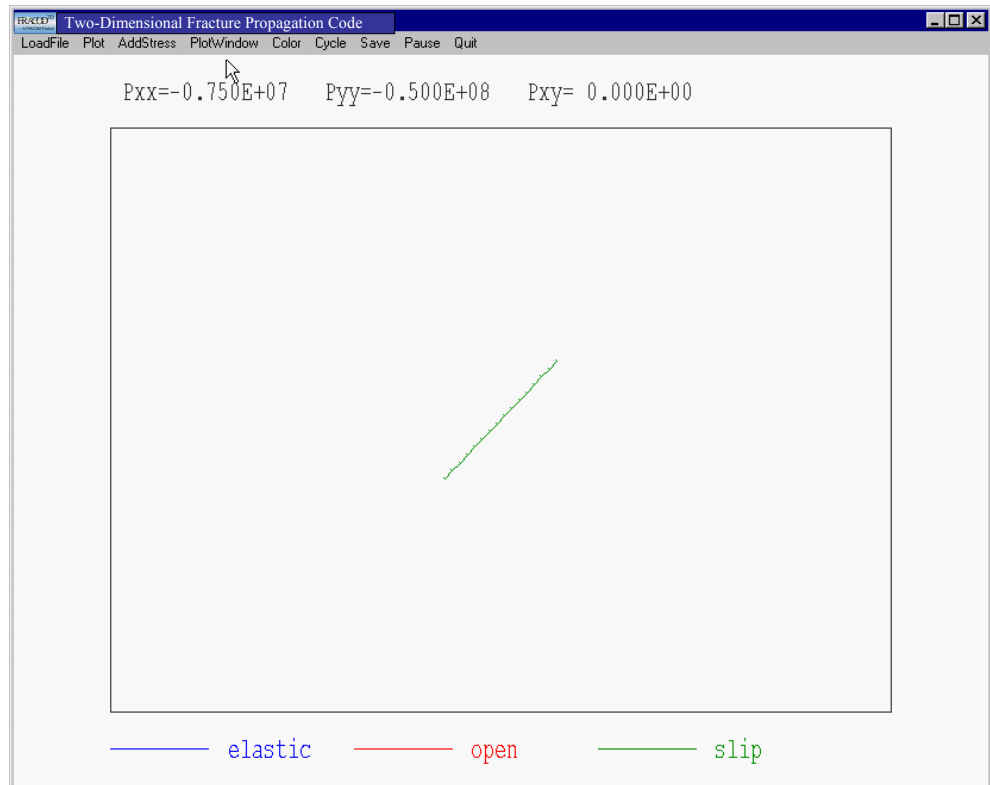
*(2) Input data*

```

-----
TITLE
Single inclined fracture subjected to biaxial compression
SYMMETRY -- Model symmetry
  0 0.00 0.00
MODULUS – Poisson's Ratio and Young's modulus
  0.25 0.40E+11
TOUGHNESS -- Gic and Giic
  50. 1000.
PROPERIES -- mat, kn, ks,phi,coh
  1 0.10E+14 0.10E+14 30.0 0.00E+00
SWINDOW -- xll,xur,yll,yur,numx,numy
  -5.00 5.00 -5.00 5.00 20 20
STRESSES -- sxx,syy,sxy
  -0.75E+07 -0.50E+08 0.00E+00
FRACTURE -- nume,xbeg,ybeg,xend,yend,kode,mat
  15 -1.000 -1.000 1.000 1.000 2 1
CYCL 1000
ENDFILE
-----

```

(3) *FRACOD model*



**Example 6 – Two inclined fractures subjected to uniaxial compression***(1) Problem definition*

Two inclined parallel fractures in an infinite rock mass are subjected to uniaxial compressive stress of 50MPa. The inclinations of the fractures are 45°. The material properties of the rock mass and fractures are the same as in Examples 1 and 3.

The fractures are found to propagate and coalesce in mode I.

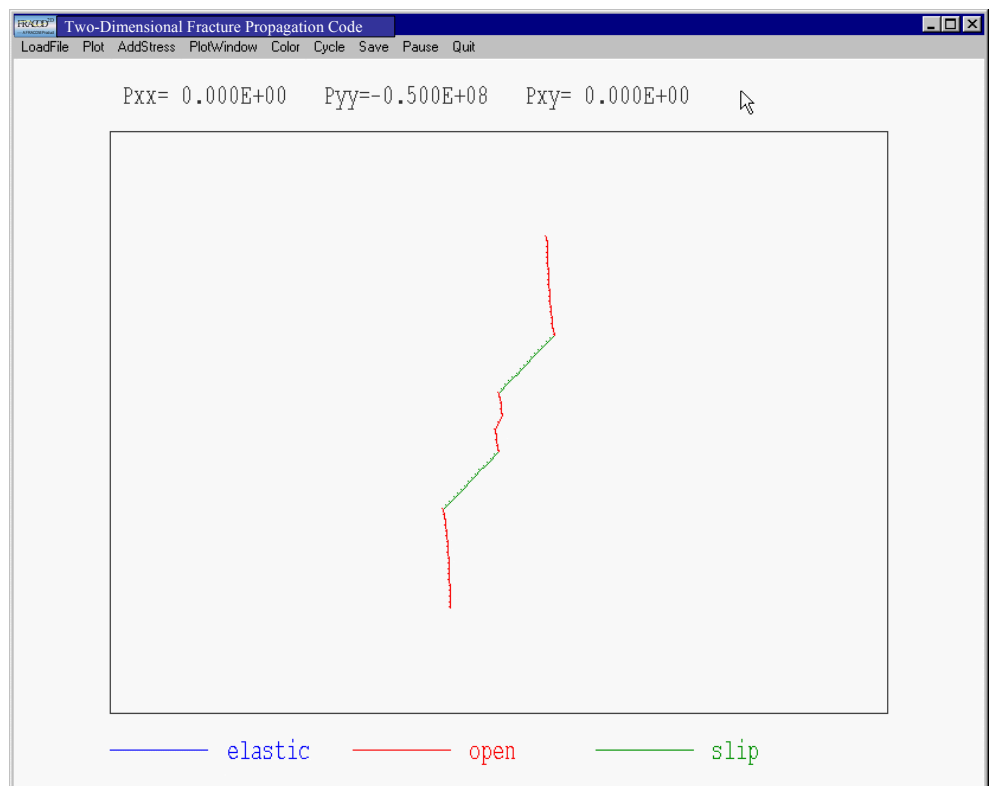
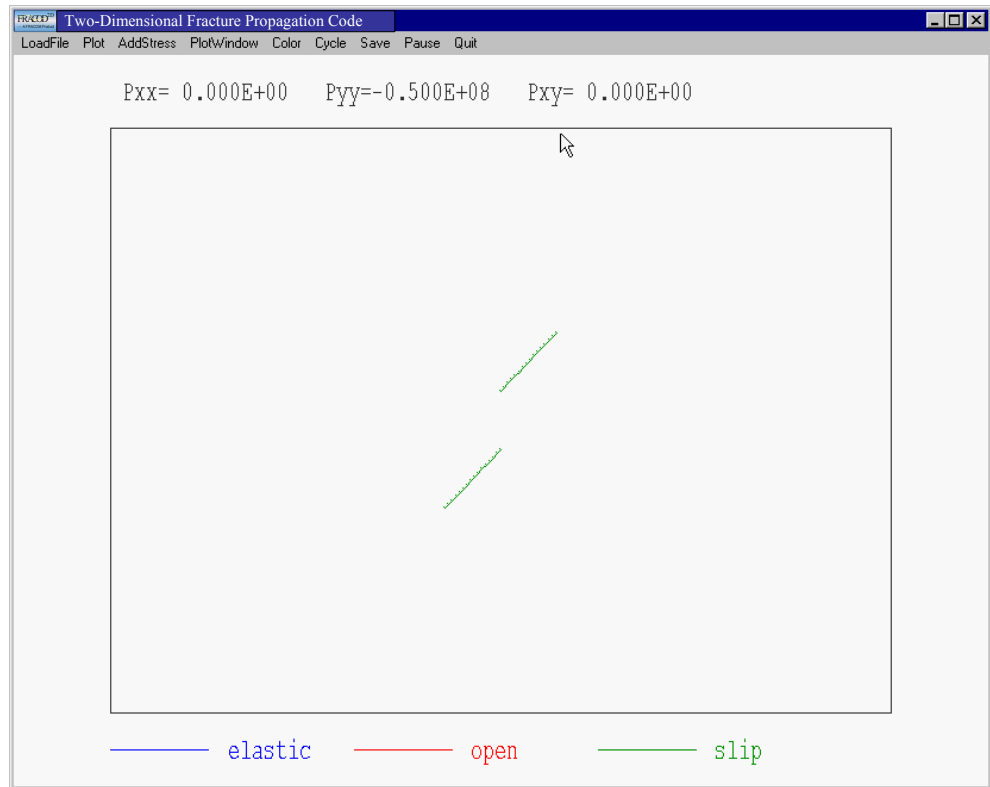
*(2) Input data*

```

-----
TITLE
Two inclined fractures subjected to uniaxial compression
SYMMETRY -- Model symmetry
  3  0.00  0.00
MODULUS – Poisson's Ratio and Young's modulus
  0.25  0.40E+11
TOUGHNESS -- Gic and Giic
  50.  1000.
PROPERIES -- mat, kn, ks,phi,coh
  1  0.10E+13  0.10E+13  30.0  0.00E+00
SWINDOW -- xll,xur,yll,yur,numx,numy
  -5.00  5.00  -5.00  5.00  30  30
STRESSES -- sxx,syy,sxy
  -0.0E+07 -0.50E+08  0.00E+00
FRACTURE -- nume,xbeg,ybeg,xend,yend,kode,mat
  15  0.000  0.500  1.000  1.500  2  1
CYCL 1000
ENDFILE
-----

```

(3) *FRACOD model*



**Example 7 – Two inclined fractures subjected to biaxial compression***(1) Problem definition*

Two inclined parallel fractures in an infinite rock mass are subjected to compressive stress of 75MPa and confining stress of 15MPa. The inclination of the fractures is 45°. The material properties of the rock mass and fractures are the same as in Examples 1 and 3.

The fractures are found to propagate and coalesce mainly in mode II. Occasional mode I propagation is also observed.

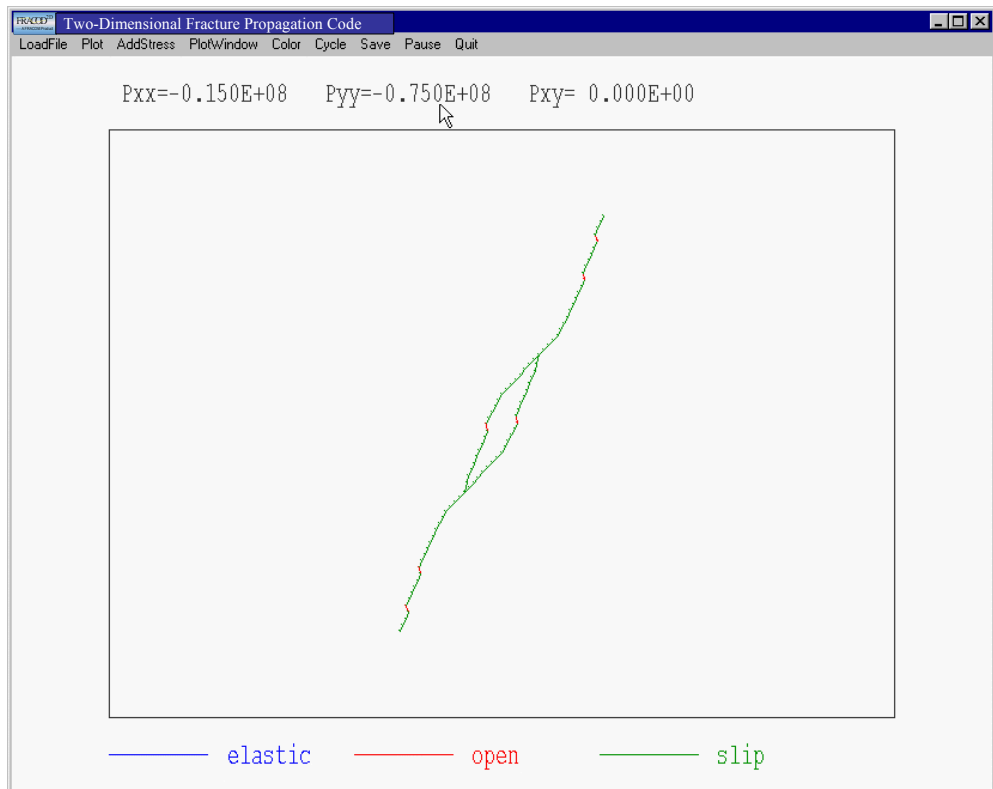
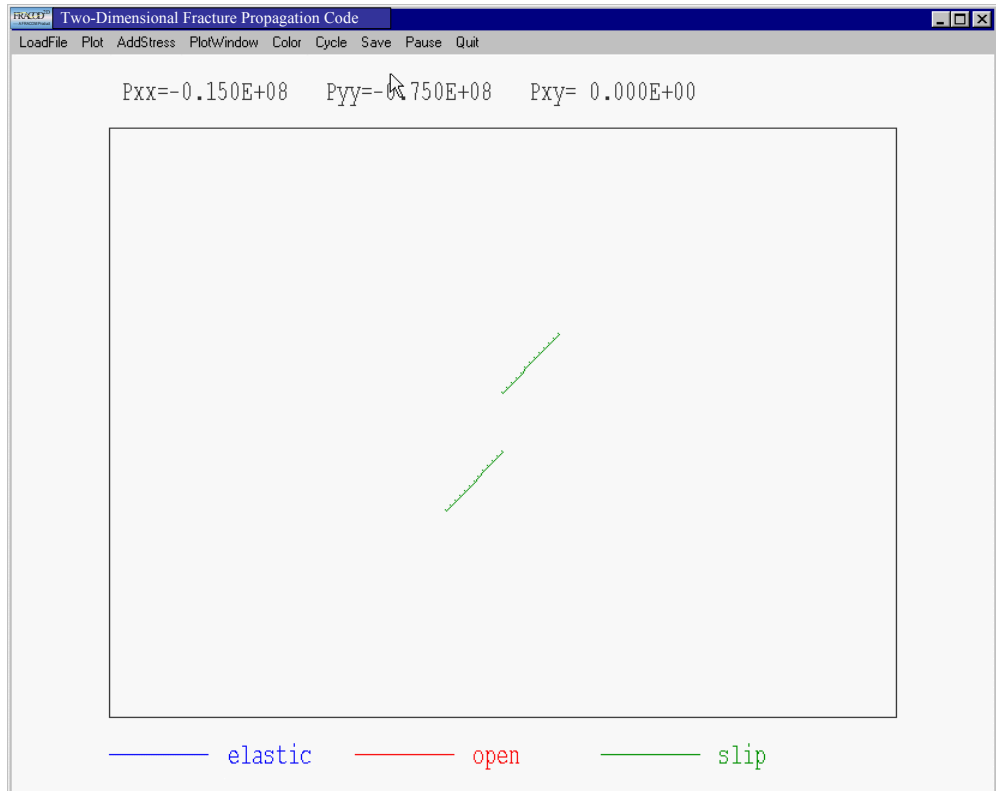
*(2) Input data*

```

-----
TITLE
Two inclined fractures subjected to biaxial compression
SYMMETRY -- Model symmetry
  3  0.00  0.00
MODULUS -- Poisson's Ratio and Young's modulus
  0.25  0.40E+11
TOUGHNESS -- Gic and Giic
  50.  1000.
PROPERIES -- mat, kn, ks,phi,coh
  1  0.10E+14  0.10E+14  30.0  0.00E+00
SWINDOW -- xll,xur,yll,yur,numx,numy
  -5.00  5.00  -5.00  5.00  30  30
STRESSES -- sxx,syy,sxy
  -0.15E+08 -0.750E+08  0.00E+00
FRACTURE -- nume,xbeg,ybeg,xend,yend,kode,mat
  12  0.000  0.500  1.000  1.500  2  1
CYCL 1000
ENDFILE
-----

```

(3) *FRACOD model*



**Example 8 – Fracture propagation from a tunnel in uniaxial compression***(1) Problem definition*

A circular tunnel with four fractures in its wall in an infinite rock mass is subjected to uniaxial compressive stress of 15MPa. The inclination of the fractures is 45°. The material properties of the rock mass and fractures are the same as in Examples 1 and 3.

The fractures are found to propagate in mode I in the direction nearly parallel to far-field compressive stress.

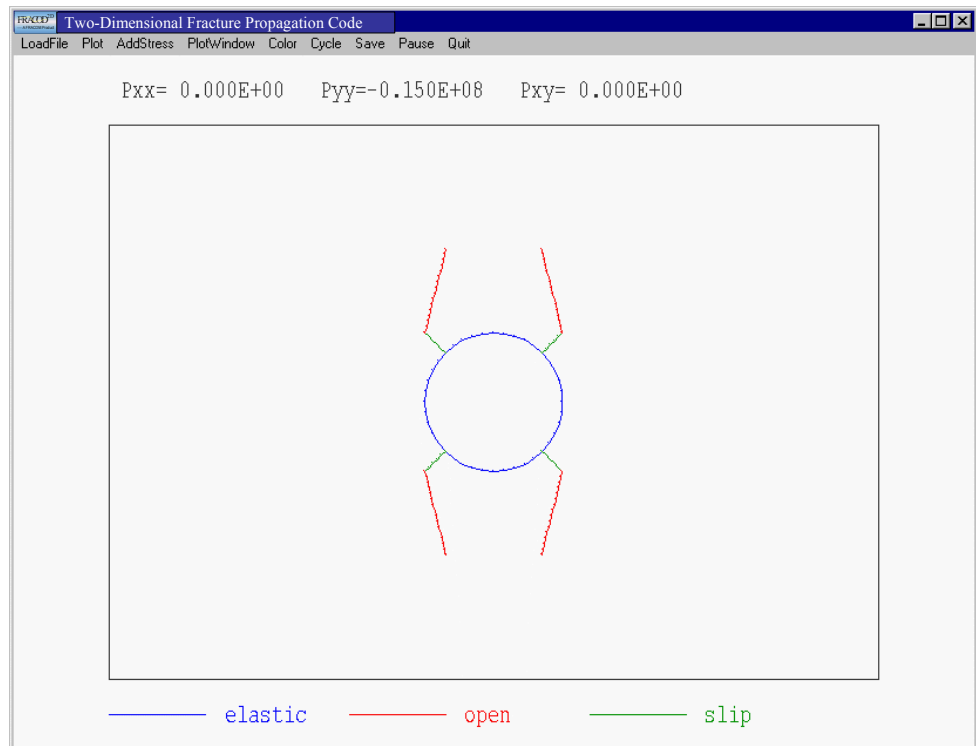
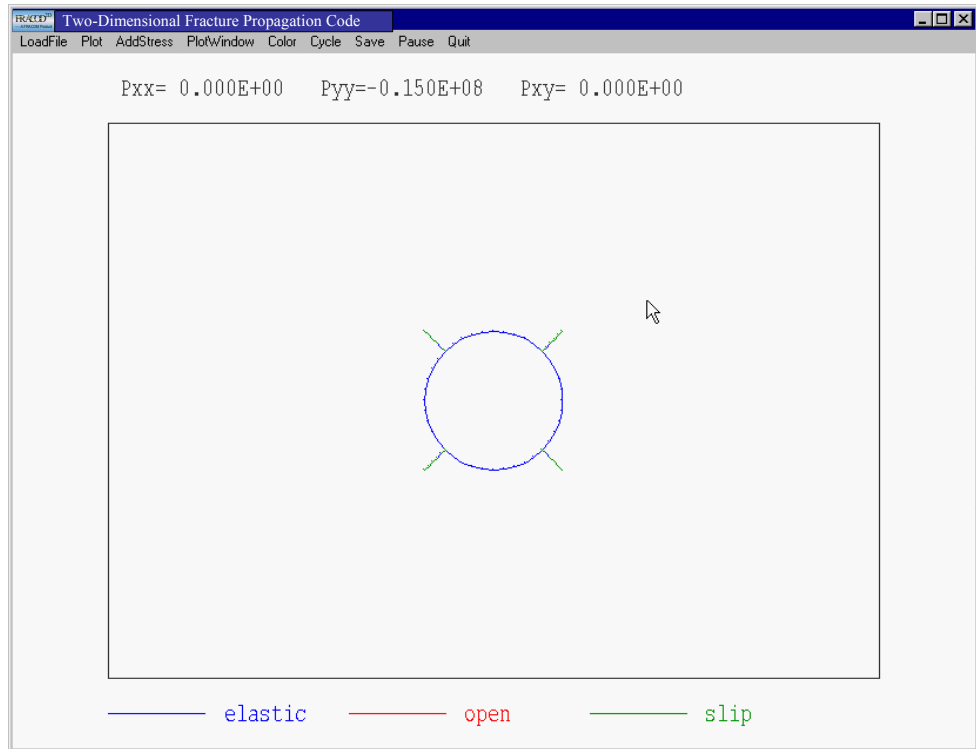
*(2) Input data*

```

-----
TITLE
A tunnel with four fractures subjected to uniaxial compression
SYMMETRY -- Model symmetry
  4  0.00  0.00
MODULUS -- Poisson's Ratio and Young's modulus
  0.25  0.40E+11
TOUGHNESS -- Gic and Giic
  50.  1000.
PROPERIES -- mat, kn, ks,phi,coh
  1  0.10E+13  0.10E+13  30.0  0.00E+00
SWINDOW -- xll,xur,yll,yur,numx,numy
  -4.00  4.00  -4.00  4.00  30  30
STRESSES -- sxx,syy,sxy
  0.00E+07 -0.15E+08  0.00E+00
FRACTURE -- nume,xbeg,ybeg,xend,yend,kode,mat
  5  0.700  0.700  1.000  1.000  2  1
ARCH -- nume,xcen,ycen,diam,ang1,ang2,kode,ss,sn
  10  0.0  0.0  2.0  0.0  90.0  1  0.00E+00  0.00E+00
CYCL 1000
ENDFILE
-----

```

(3) *FRACOD model*



**Example 9 – Fracture propagation from a tunnel under internal hydraulic pressure**

(1) *Problem definition*

A circular tunnel with four fractures in its wall in an infinite rock mass is subjected to internal hydraulic pressure of 50MPa. The in situ stresses (far-field stresses) in the rock mass are  $P_{xx}=P_{yy}=10\text{MPa}$ . The inclination of the fractures is  $45^\circ$ . The material properties of the rock mass and fractures are the same as in Examples 1 and 3.

The fractures are found to propagate in mode I in radial direction.

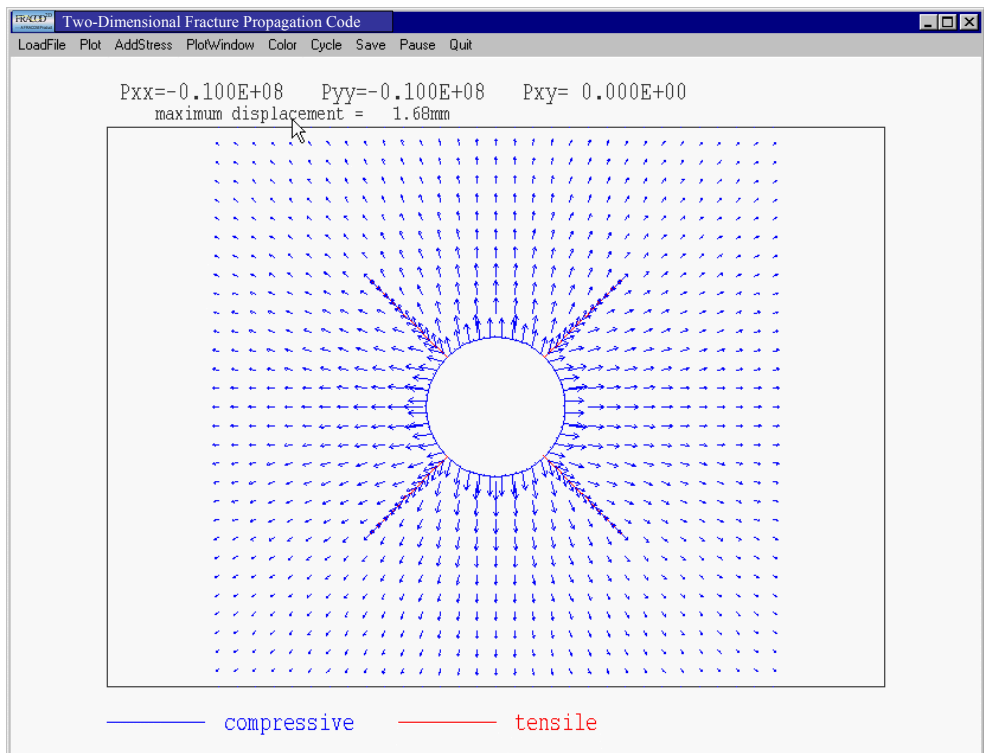
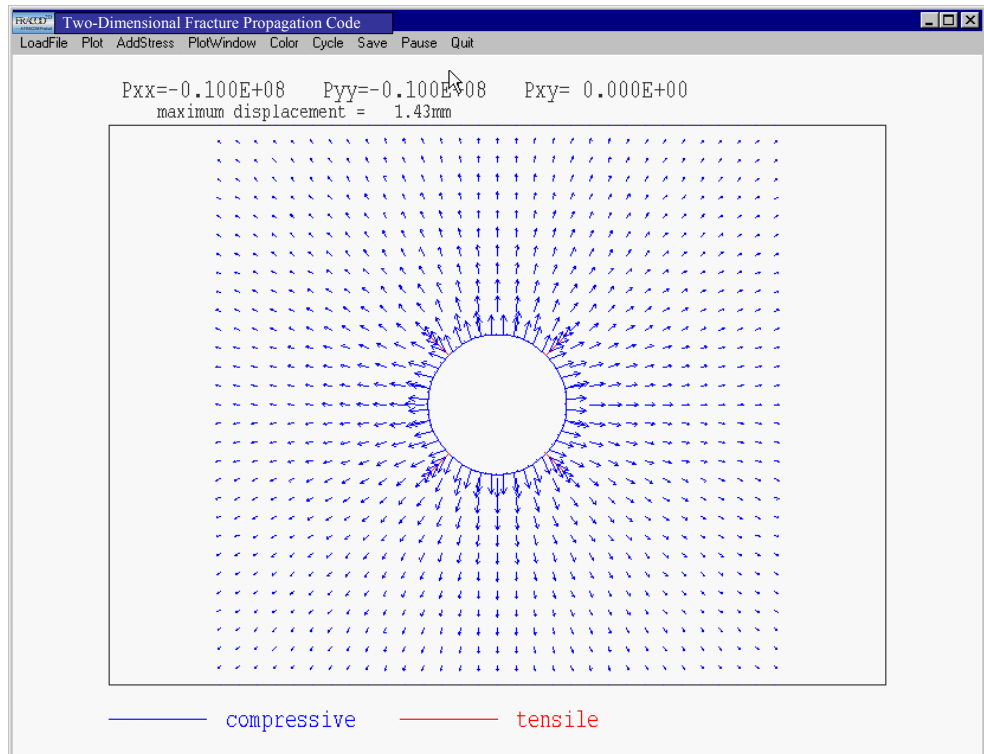
(2) *Input data*

```

-----
TITLE
A tunnel with four fractures subjected to internal hydraulic pressure
SYMMETRY -- Model symmetry
  4  0.00  0.00
MODULUS – Poisson's Ratio and Young's modulus
  0.25  0.40E+11
TOUGHNESS -- Gic and Giic
  50.  1000.
PROPERIES -- mat, kn, ks,phi,coh
  1  0.10E+13  0.10E+13  30.0  0.00E+00
SWINDOW -- xll,xur,yll,yur,numx,numy
  -4.00  4.00  -4.00  4.00  30  30
STRESSES -- sxx,syy,sxy
  -10.0E+06  -10.00E+06  0.00E+00
FRACTURE -- nume,xbeg,ybeg,xend,yend,kode,mat
  3  0.700  0.700  1.000  1.000  2  1
ARCH -- nume,xcen,ycen,diam,ang1,ang2,kode,ss,sn
  10  0.0  0.0  2.0  0.0  90.0  1  0.00E+00  -50.E+06
CYCL 1000
ENDFILE
-----

```

(3) *FRACOD model*



**Example 10 – Simple fracture propagation to form borehole breakouts***(1) Problem definition*

A circular borehole with four fractures in its wall in an infinite rock mass is subjected to compressive stress of 50MPa and confining stress of 10MPa. The borehole is also subjected to an internal hydraulic pressure of 10MPa. The inclination of the fractures is  $-45^\circ$ . The material properties of the rock mass and fractures are the same as in Examples 1 and 3.

The fractures are found to propagate toward each other in mode II and finally form borehole breakouts.

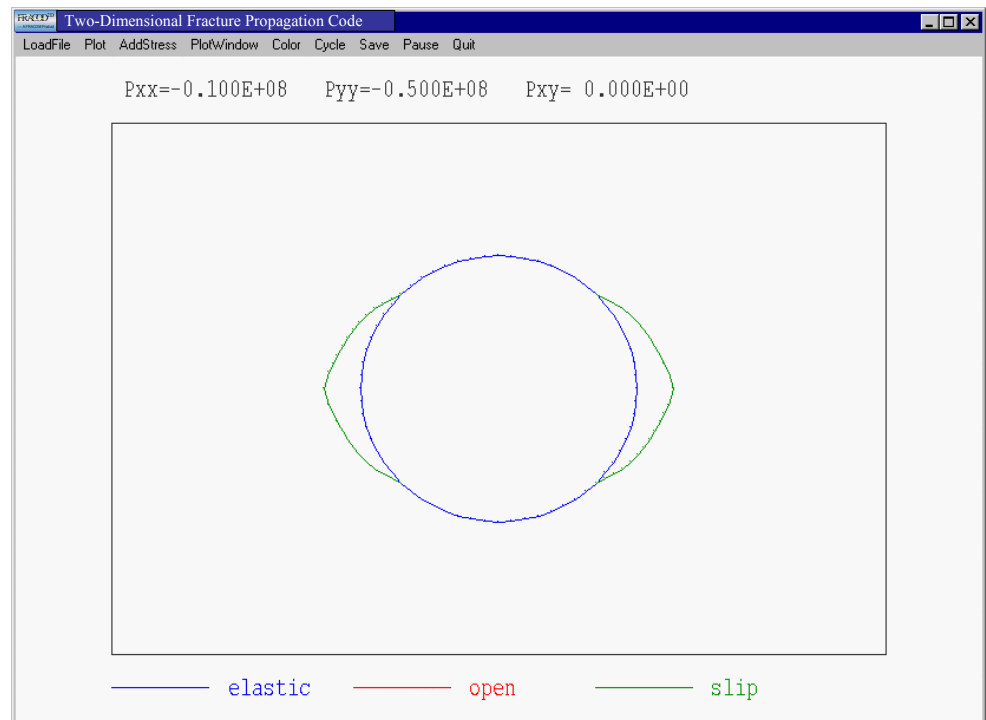
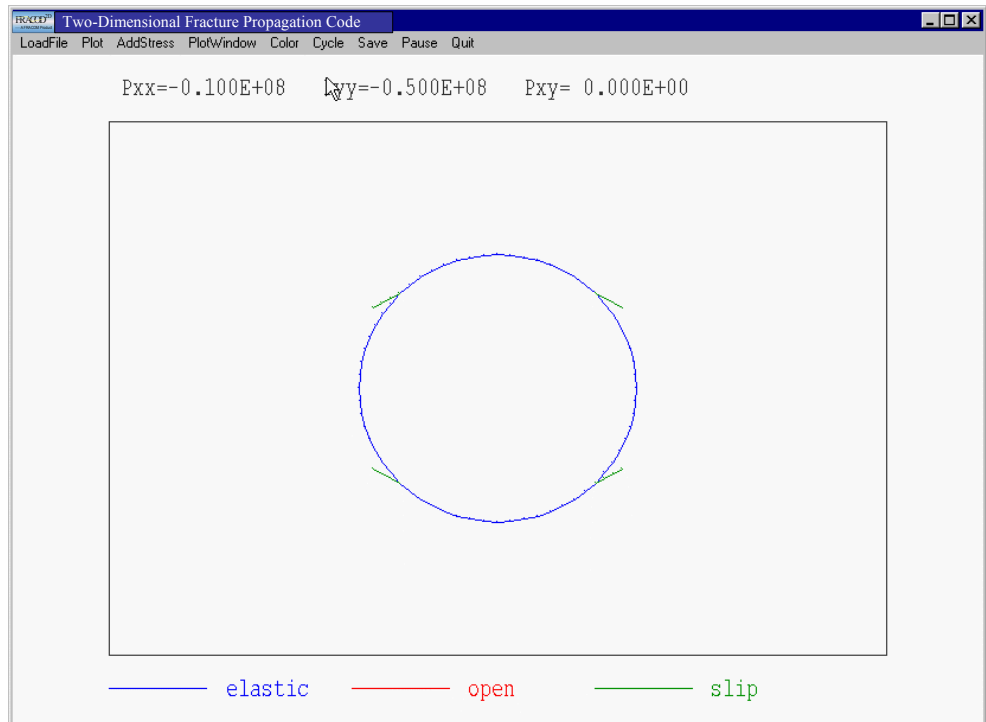
*(2) Input data*

```

-----
TITLE
Fracture propagation to form borehole breakouts
SYMMETRY -- Model symmetry
  4  0.00  0.00
MODULUS -- Poisson's Ratio and Young's modulus
  0.25  0.40E+11
TOUGHNESS -- Gic and Giic
  50.  1000.
PROPERIES -- mat, kn, ks,phi,coh
  1  0.10E+13  0.10E+13  30.0  0.00E+00
SWINDOW -- xll,xur,yll,yur,numx,numy
  -2.00  2.00  -2.00  2.00  30  30
STRESSES -- sxx,syy,sxy
  -10.0E+06  -50.00E+06  0.00E+00
FRACTURE -- nume,xbeg,ybeg,xend,yend,kode,mat
  3  0.700  0.700  0.90  0.60  2  1
ARCH -- nume,xcen,ycen,diam,ang1,ang2,kode,ss,sn
  15  0.0  0.0  2.0  0.0  90.0  1  0.00E+00  -10.E+06
CYCL 1000
ENDFILE
-----

```

(3) *FRACOD model*



**Example 11 – Complex fracture propagation to form borehole breakouts**

(1) *Problem definition*

A circular borehole with hoop cracks in the borehole wall in an infinite rock mass is subjected to compressive stress of 60MPa and confining stress of 30MPa. The borehole is also free from any internal hydraulic pressure. The cracks are parallel to the borehole walls. The material properties of the rock mass and fractures are the same as in Examples 1 and 3.

The cracks are found to propagate and coalesce in a complex pattern. Both mode I and mode II failures are involved. The fracture propagation finally forms breakouts which have a failure pattern similar to that observed in the laboratory tests and field observations.

(2) *Input data*

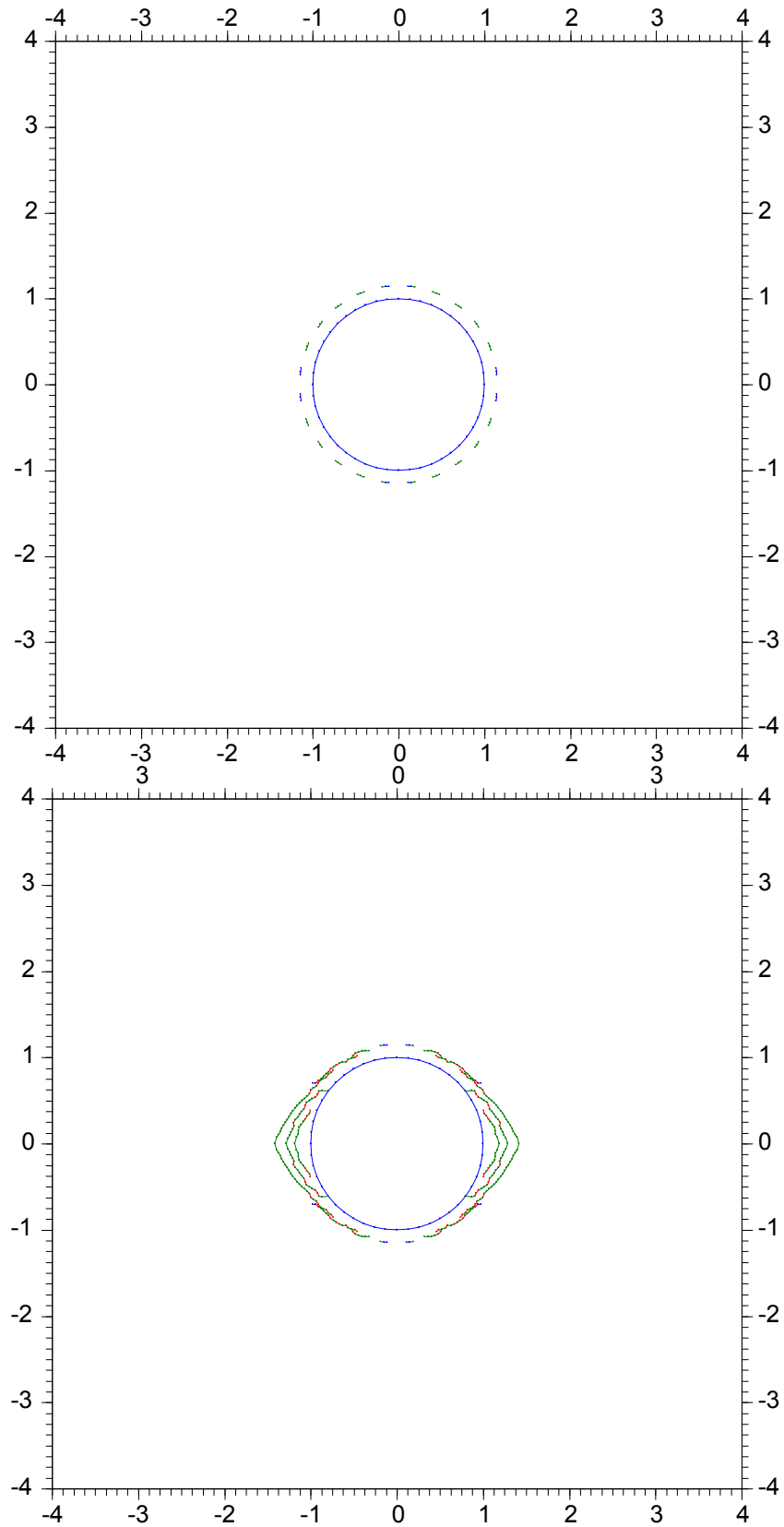
```

-----
TITLE
Complex fracture propagation to form borehole breakouts
SYMMETRY -- Model symmetry
  4 0.00 0.00
MODULUS – Poisson's Ratio and Young's modulus
0.25 0.40E+11
TOUGHNESS -- Gic and Giic
  50. 1000.
PROPERIES -- mat, kn, ks,phi,coh
  1 0.10E+13 0.10E+13 30.0 0.00E+00
SWINDOW -- xll,xur,yll,yur,numx,numy
  -2.00 2.00 -2.00 2.00 30 30
STRESSES -- sxx,syy,sxy
  -10.0E+06 -50.00E+06 0.00E+00
STRESSES -- sxx,syy,sxy
  -3.0E+08 -0.60E+08 0.00E+00
ARCH -- nume,xcen,ycen,diam,ang1,ang2,kode,ss,sn
12 0.0 0.0 2.0 0.0 90.0 1 0.00E+00 -0.00E+06
FRACTURE -- nume,xbeg,ybeg,xend,yend,kode,mat
2 1.144703678 0.11024287 1.134231801 0.189784673 5 1
FRACTURE -- nume,xbeg,ybeg,xend,yend,kode,mat
2 1.077165893 0.402757543 1.046463904 0.476878704 5 1
FRACTURE -- nume,xbeg,ybeg,xend,yend,kode,mat
2 0.936221036 0.667824956 0.887381223 0.73147424 5 1
FRACTURE -- nume,xbeg,ybeg,xend,yend,kode,mat
2 0.731474264 0.887381204 0.667824981 0.936221018 5 1
FRACTURE -- nume,xbeg,ybeg,xend,yend,kode,mat
2 0.476878732 1.046463891 0.402757572 1.077165882 5 1
FRACTURE -- nume,xbeg,ybeg,xend,yend,kode,mat
2 0.189784703 1.134231796 0.1102429 1.144703675 5 1
CYCL 10000
ENDFILE
-----

```

(3) *FRACOD model*

Complex fracture propagation to form borehole breakouts

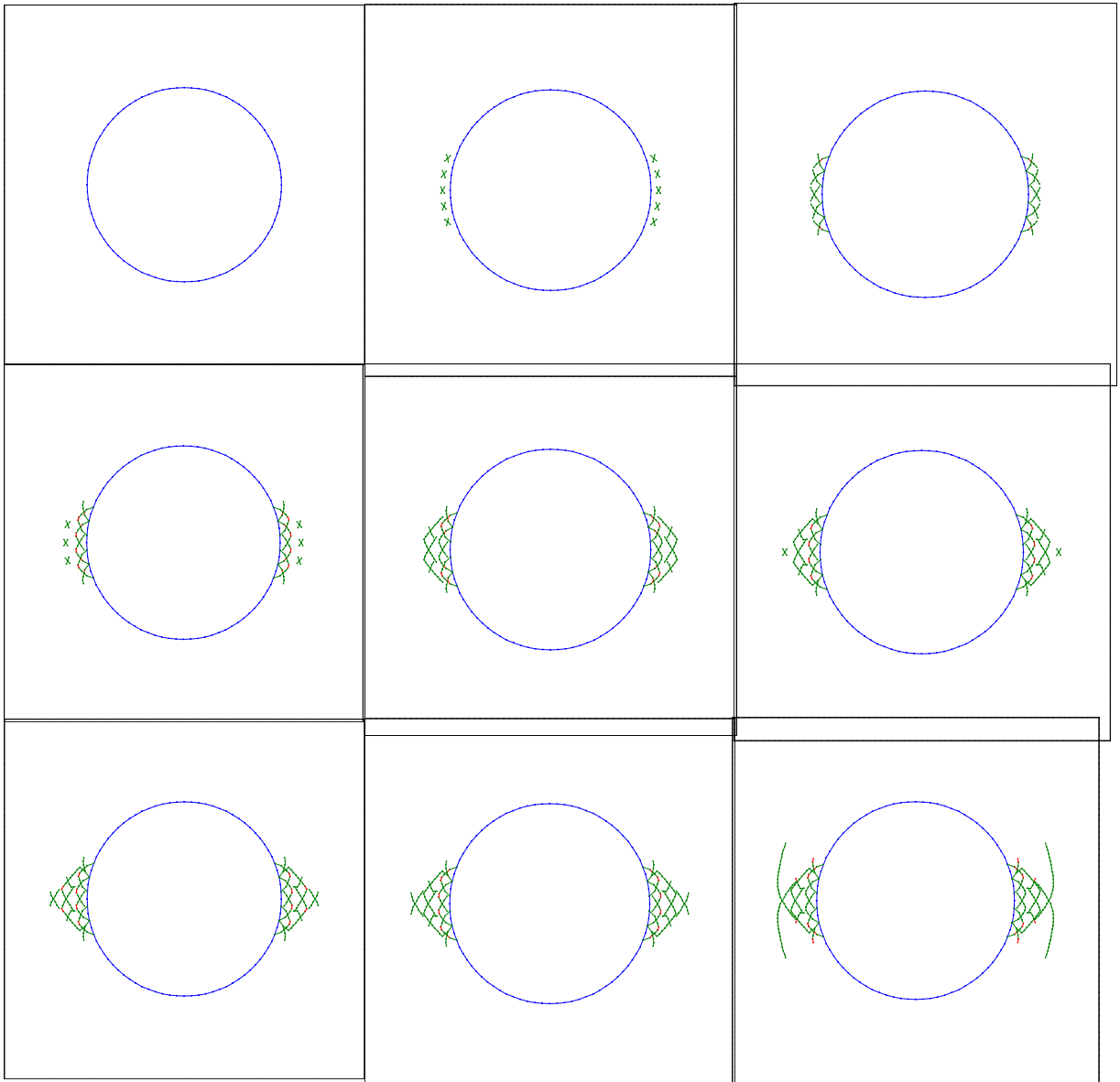


**Example 12 – Fracture initiation and propagation to form borehole breakouts**

A circular borehole in an infinite rock mass is subjected to compressive stress and confining stress. The borehole is also subjected to internal hydraulic pressure. No cracks exist in the borehole walls. The material properties of the rock mass and fractures are given below:

- $K_{IC}=1.08 \text{ MPa m}^{1/2}$ ;  $K_{IIC}= K_{IC}$
- Tensile strength = 7MPa
- Compressive strength  $\sigma_c=28\text{MPa}$
- Failure criterion  $(\sigma_1)^2 = 200*(\sigma_3 + 3.95)$ ;
- $E=55\text{GPa}$ ,  $\nu=0.25$
- Insitu stresses:  $\sigma_H=36\text{MPa}$ ,  $\sigma_h =45\text{MPa}$ , fluid pressure  $\sigma_p =18\text{MPa}$
- Fracture contact properties:  $K_s=K_n=10e4\text{GPa/m}$ ; friction angle=0 degrees, cohesion=0
- Borehole Diameter =0.216m

Fracture initiation is predicted inside the borehole wall. The new fractures propagate and coalesce while new fractures continue to initiate. The process continues and finally forms borehole breakouts, see the plots below.



## APENDIX III – DETERMINATION OF THE DIRECTION OF SHEAR FRACTURES

When a fracture propagates in shear at an existing fracture tip, there are always two conjugate candidate propagation directions in which the shear stress reaches the maximum. The same mechanism causes the phenomenon that two conjugate failure planes often occur during triaxial compression tests of rock samples in laboratory. In most cases, however, shear failure takes place only in one direction because the friction resistant is much higher in the conjugate direction due to higher normal stress. Figure A1 shows such a situation, where the candidate direction (1) is the sole fracture propagation direction due to its lower friction resistant than the direction (2).

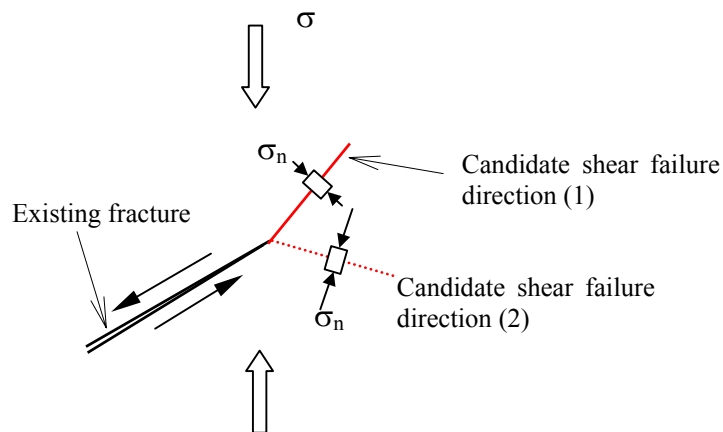


Figure A1. Two candidate directions of shear failure. Direction (1) is the favourable one due to its low shear resistant.

In other cases, shear failure could in theory occur in both directions if the shear resistant happens to be same or similar in the two directions of the maximum shear stress. This is particularly true when the shear failure initiates from an open fracture tip, see Figure A2. In Figure A2, the shear fracture can in theory propagate in both directions (1) and (2) since both directions has the same shear stress and normal stress. In reality, however, a fracture propagation in direction (2) is rarely observed, simply because it creates a conflicting shear movement against the existing fracture. A fracture initiation in direction (2) may occur, but its odd shear direction prevents it from growing longer to form a sustainable shear fracture propagation. In this case the true shear fracture propagation has to be the direction (1) in which the shear movement of the new fracture is consistent with the existing fractures.

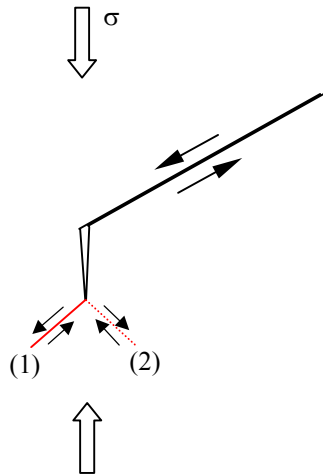


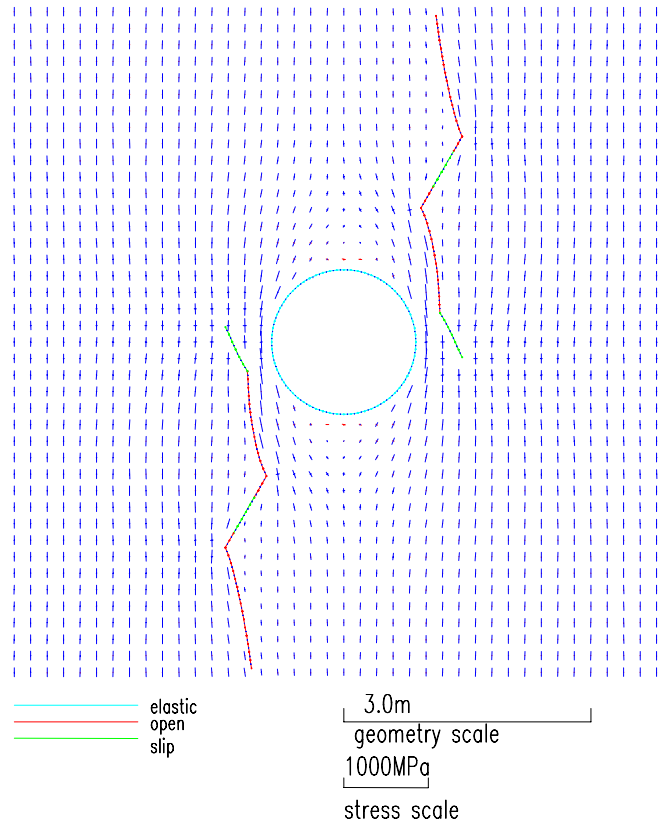
Figure A2. Two candidate directions for shear failure. Only in direction (1) can a sustainable fracture growth occur.

To accurately model the shear fracture direction for the cases as shown in Figure A2, we need to ensure that the FRACOD code can intelligently select the physically correct direction (1). This has been done by introducing a criterion to eliminate the shear failure direction which creates conflicting shear movement against the pre-existing fracture. Without such a criterion, the FRACOD code can only randomly select one direction between the two candidate directions, and in some cases gives an incorrect prediction.

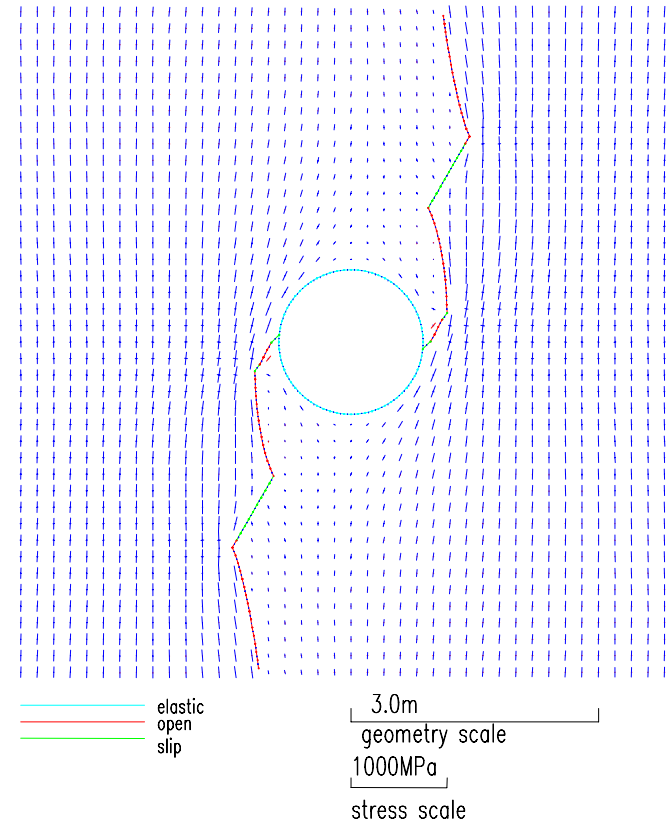
Figure A3 demonstrates the improvement after introducing the direction selection criterion in the FRACOD code. In Figure 3, a borehole and two inclined fractures are modelled to study whether the fractures propagate to the borehole in uniaxial compression. The two figures in Figure 3 show two different paths of fracture propagation predicted by FRACOD before and after the introduction of the criterion. Clearly, the prediction obtained with the direction selection criterion is more reasonable as one would expect such fractures normally propagate to the borehole rather than deviating away from the borehole.

far field  $s_{xx}= 0$ .  $s_{yy}=100$   $s_{xy}= 0$ . (MPa)  
 maximum principal stress = 253.4MPa

far field  $s_{xx}= 0$ .  $s_{yy}=100$   $s_{xy}= 0$ . (MPa)  
 maximum principal stress = 223.3MPa



(a) before



(b) after

Figure A3. Two fracture propagation paths predicted by FRACOD before and after the shear direction selection criterion was introduced.

